

N₂ fixation in the Mediterranean Sea related to the composition of the diazotrophic community, and impact of dust under present and future environmental conditions

Céline Ridame¹, Julie Dinasquet^{2,3}, Søren Hallstrøm⁴, Estelle Bigeard⁵, Lasse Riemann⁴, France Van Wambeke⁶, Matthieu Bressac⁷, Elvira Pulido-Villena⁶, Vincent Taillandier⁷, Frédéric Gazeau⁷, Antonio Tovar-Sanchez⁸, Anne-Claire Baudoux⁵, Cécile Guieu⁷

¹ Sorbonne University, CNRS, IRD, LOCEAN: Laboratoire d'Océanographie et du Climat: Expérimentation et Approches Numériques, UMR 7159, 75252 Paris Cedex 05, France

² Scripps Institution of Oceanography, University of California San Diego, USA

³ Sorbonne University, CNRS, Laboratoire d'Océanographie Microbienne, LOMIC, 66650 Banyuls-sur-Mer, France

⁴ Marine Biology Section, Department of Biology, University of Copenhagen, 3000 Helsingør, Denmark

⁵ Sorbonne University, CNRS, Station Biologique de Roscoff, UMR 7144 Adaptation et Diversité en Milieu Marin, France

⁶ Aix-Marseille Université, Université de Toulon, CNRS/INSU, IRD, Mediterranean Institute of Oceanography (MIO), UM 110, 13288, Marseille, France

⁷ Sorbonne Université, CNRS, Laboratoire d'Océanographie de Villefranche, LOV, 06230 Villefranche-sur-Mer, France

⁸ Department of Ecology and Coastal Management, Institute of Marine Sciences of Andalusia (CSIC), 11510 Puerto Real, Cádiz, Spain

Correspondence to: Céline Ridame (celine.ridame@locean.ipsl.fr)

Abstract. N₂ fixation rates were measured in the 0-1000 m layer at 13 stations located in the open western and central Mediterranean Sea (MS) during the PEACETIME cruise (late spring 2017). While the spatial variability of N₂ fixation was not related to Fe, P nor N stocks, the surface composition of the diazotrophic community indicated a strong longitudinal gradient increasing eastward for the relative abundance of non-cyanobacterial diazotrophs (NCD) (mainly γ -Proteobacteria) and conversely decreasing eastward for UCYN-A (mainly -A1 and -A3) as did N₂ fixation rates. UCYN-A4 and -A3 were identified for the first time in the MS. The westernmost station influenced by Atlantic waters, and characterized by highest stocks of N and P, displayed a patchy distribution of diazotrophic activity with an exceptionally high rate in the euphotic layer of 72.1 nmol N L⁻¹ d⁻¹, which could support up to 19 % of primary production. At this station at 1%PAR depth, UCYN-A4 represented up to 94 % of the diazotrophic community. These *in situ* observations of greater relative abundance of UCYN-A at stations with higher nutrient concentrations and dominance of NCD at more oligotrophic stations suggest that nutrient conditions - even in the nanomolar range - may determine the composition of diazotrophic communities and in turn N₂ fixation rates. The impact of Saharan dust deposition on N₂ fixation and diazotrophic communities was also investigated, under present and future projected conditions of temperature and pH during short term (3-4 days) experiments at three

35 stations. New nutrients from simulated dust deposition triggered a significant stimulation of N₂ fixation (from 41 % to 565
36 %). The strongest increase in N₂ fixation was observed at the stations dominated by NCD and did not lead on this short time
37 scale to change in the diazotrophic community composition. Under projected future conditions, N₂ fixation was either
38 increased or unchanged; in that later case this was probably due to a too low nutrient bioavailability or an increased grazing
39 pressure. The future warming and acidification likely benefited NCD (*Pseudomonas*) and UCYN-A2 while disadvantaged
40 UCYN-A3 without knowing which effect (alone or in combination) is the driver, especially since we do not know the
41 temperature optima of these species not yet cultivated as well as the effect of acidification.

42 **1. Introduction**

43 The Mediterranean Sea (MS) is considered as one of the most oligotrophic regions of the world's ocean (Krom et al., 2004;
44 Bosc et al., 2004). It is characterized by a longitudinal gradient in nutrient availability, phytoplanktonic biomass and primary
45 production (PP) decreasing eastward (Manca et al., 2004; D'Ortenzio and Ribera d'Alcalà, 2009; Ignatiades et al., 2009;
46 Siokou-Frangou et al., 2010; El Hourany et al., 2019). From May to October, the upper water column is well-stratified
47 (D'Ortenzio et al., 2005), and the sea surface mixed layer (SML) becomes nutrient-depleted leading to low PP (e.g. Lazzari
48 et al., 2012). Most measurements of N₂ fixation during the stratified period have shown low rates ($\leq 0.5 \text{ nmol N L}^{-1} \text{ d}^{-1}$) in
49 surface waters of the open MS (Ibello et al., 2010; Bonnet et al., 2011; Yogeve et al., 2011; Ridame et al., 2011; Rahav et al.,
50 2013a; Benavides et al., 2016) indicating that N₂ fixation represents a minor source of bioavailable nitrogen in the MS
51 (Krom et al., 2010; Bonnet et al., 2011). These low rates are likely related to the extremely low bioavailability in dissolved
52 inorganic phosphorus (DIP) (Rees et al., 2006; Ridame et al., 2011). The high concentrations of dissolved iron (DFe) in the
53 SML due to accumulated atmospheric Fe deposition (Bonnet and Guieu 2006; Tovar-Sánchez et al. 2020; Bressac et al.,
54 2021), suggest that the bioavailability of Fe is not a controlling factor of N₂ fixation (Ridame et al., 2011). Occasionally,
55 high N₂ fixation rates have been reported locally in the northwestern ($17 \text{ nmol N L}^{-1} \text{ d}^{-1}$; Garcia et al., 2006) and eastern MS
56 ($129 \text{ nmol N L}^{-1} \text{ d}^{-1}$; Rees et al., 2006). Usually, the low N₂ fixation rates in the Mediterranean offshore waters are associated
57 with low abundance of diazotrophs, mainly dominated by unicellular organisms (Man-Aharonovich et al., 2007; Yogeve et
58 al., 2011; Le Moal et al., 2011). Unicellular diazotrophs from the photo-heterotrophic group A (UCYN-A, Zehr et al., 1998)
59 largely dominated the cyanobacteria assemblage in the MS (Le Moal et al., 2011), and very low concentrations of
60 filamentous diazotrophic cyanobacteria have only been recorded in the eastern basin (Bar-Zeev et al., 2008; Le Moal et al.,
61 2011; Yogeve et al., 2011). The UCYN-A cluster consist of four sublineages: UCYN-A1, -A2, -A3 and -A4 (Thompson et al.,
62 2014; Farnelid et al., 2016; Turk Kubo et al., 2017; Cornejo-Castillo et al., 2019), of which only UCYN-A1 and -A2 have
63 been previously detected in the MS (Man-Aharonovich et al., 2007; Martinez-Perez et al., 2016; Pierrela Karlusich et al.,
64 2021). Heterotrophic diazotrophs are widely distributed over the offshore surface waters (Le Moal et al, 2011), and the
65 decreasing eastward gradient of surface N₂ fixation rate could be related to a predominance of photo-autotrophic diazotrophs
66 in the western basin and a predominance of heterotrophic diazotrophs in the eastern one (Rahav et al. 2013a).

67 The MS is strongly impacted by periodic dust events, originating from the Sahara, which have been recognized as a
68 significant source of macro- and micronutrients, to the nutrient depleted SML during stratified periods (Guieu and Ridame,
69 2020 and references therein; Mas et al., 2020). Results from Saharan dust seeding experiments during open sea microcosms
70 and coastal mesocosms in the MS, showed stimulation of both PP (Herut et al., 2005; Ternon et al., 2011; Ridame et al.,
71 2014 ; Herut et al., 2016) and heterotrophic bacterial production (BP) (Pulido-Villena et al., 2008, 2014; Lekunberri et al.,
72 2010; Herut et al., 2016). Experimental Saharan dust seeding was also shown to enhance N₂ fixation in the western and
73 eastern MS (Ridame et al., 2011; Ternon et al., 2011; Ridame et al., 2013; Rahav et al., 2016a) and to alter the composition
74 of the diazotrophic community (Rahav et al., 2016a), as also shown in the tropical North Atlantic (Langlois et al., 2012).

75 The MS has been identified as one of the primary hot-spots for climate change (Giorgi, 2006). Future sea surface warming
76 and associated increase in stratification (Somot et al., 2008) might reinforce the importance of atmospheric inputs as a source
77 of new nutrients for biological activities during that season, including diazotrophic microorganisms. This fertilizing effect
78 could also be enhanced by the expected decline in pH (Mermex Group, 2011), which could increase the nutrient dust
79 solubility in seawater. Under nutrient depleted conditions, predicted elevated temperature and CO₂ concentration favor the
80 growth and N₂ fixation of the filamentous cyanobacteria *Trichodesmium* and of the photo-autotrophic UCYN-B and -C
81 (Webb et al., 2008; Hutchins et al., 2013; Fu et al., 2008, 2014; Eichner et al., 2014; Jiang et al., 2018), whereas effects on
82 UCYN-A and non-cyanobacterial diazotrophs (NCD) are uncertain.

83 In this context, the first objective of this study is to investigate during the season characterized by strong stratification and
84 low productivity, the spatial variability of N₂ fixation rates in relation to nutrient availability and diazotrophic community
85 composition. The second objective was to study, for the first time, the impact of a realistic Saharan deposition event in the
86 open MS, on N₂ fixation rates and diazotrophic communities composition under present and realistic projected conditions of
87 temperature and pH for 2100.

88

89 **2. Materials and Methods**

90 **2.1 Oceanographic cruise**

91 All data were acquired during the PEACETIME cruise (ProcEss studies at the Air-sEa Interface after dust deposition in the
92 MEditerranean sea) in the western and central MS on board the R/V *Pourquoi Pas ?* from May 10 to June 11, 2017
93 (<http://peacetime-project.org/>) (see the detailed description in Guieu et al., 2020). The cruise track including ten short
94 stations (ST1 to ST10) and three long stations (TYR, ION and FAST) is shown in Fig.1 (coordinates in Table S1). Stations 1
95 and 2 were located in the Liguro-Provencal basin; Stations 5, 6, and TYR, in the Tyrrhenian Sea; Stations 7, 8, and ION in
96 the Ionian Sea; and Stations 3, 4, 9, 10 and FAST in the Algerian basin.

97

98 **2.2 Dust seeding experiments**

99 Experimental dust seedings into six large tanks were conducted at each of the three long stations (TYR, ION and FAST),
100 under present and future conditions of temperature and pH. Based on previous studies, the location of these stations was

101 chosen based on several criteria including because they represent three main bioregions of the MS (Guieu et al., 2020, their
102 Fig. S1). They are located along the longitudinal gradient in biological activity, including the activity of diazotrophs
103 decreasing eastward (Bonnet et al., 2011; Rahav et al., 2013a). The experimental setup is fully described in a companion
104 paper (Gazeau et al., 2021a). Briefly, six climate reactors (volume of about 300 L) made in high density polyethylene were
105 placed in a temperature-controlled container, and covered with a lid equipped with LEDs to reproduce natural light cycle.
106 The tanks were filled with unfiltered surface seawater collected at ~5m with a peristaltic pump at the end of the day (T-12h)
107 before the start of the experiments the next morning (T0). Two replicate tanks were amended with mineral Saharan dust
108 (Dust treatments D1 and D2) simulating a high but realistic atmospheric dust deposition of 10 g m^{-2} (Guieu et al., 2010b).
109 Two other tanks were also amended with Saharan dust (same dust flux as in the Dust treatment) under warmer ($\sim +3^\circ \text{ C}$) and
110 more acidic water conditions ($\sim -0.3 \text{ pH unit}$) (Greenhouse treatments G1 and G2). This corresponds to the IPCC projections
111 for 2100 under RCP8.5 (IPCC 2019). Seawater in G1 and G2 was warmed overnight to reach $+3^\circ \text{ C}$ and acidified through
112 the addition of CO_2 -saturated $0.2 \text{ }\mu\text{m}$ -filtered seawater ($\sim 1.5 \text{ L}$ in 300 L). The difference in temperature between G
113 (Greenhouse) tanks and other tanks (C, Controls and D, Dust) was $+3^\circ \text{ C}$, $+3.2^\circ \text{ C}$ and $+3.6^\circ \text{ C}$ at TYR, ION and FAST,
114 respectively, and the decrease in pH was -0.31 , -0.29 and -0.33 at TYR, ION and FAST, respectively (Gazeau et al., 2021a).
115 Two tanks were filled with untreated water (Controls C1 and C2). The experiment at TYR and ION lasted three days while
116 the experiment at FAST lasted four days. The sampling session took place every morning at the same time over the duration
117 of the experiments.

118 The fine fraction ($< 20 \text{ }\mu\text{m}$) of a Saharan soil collected in southern Tunisia used in this study, has been previously used for
119 the seeding of mesocosms in the frame of the DUNE project (a DUst experiment in a low-Nutrient, low-chlorophyll
120 Ecosystem). Briefly, the dust was previously subjected to physico-chemical transformations mimicking the mixing between
121 dust and pollution air masses during atmospheric transport (see details in Desboeufs et al, 2001; Guieu et al., 2010b). This
122 dust contained $0.055 \pm 0.003 \%$ of P, $1.36 \pm 0.09 \%$ of N, and $2.26 \pm 0.03 \%$ of Fe, in weight (Desboeufs et al., 2014). Right
123 before the artificial seeding, the dust was mixed with 2 L of ultrapure water in order to mimic a wet deposition event and
124 sprayed at the surface of the climate reactors D and G. The succession of operations is fully described in Gazeau et al.,
125 (2021a, see their Table 1).

126

127 **2.3 N_2 fixation and primary production**

128 All materials were acid washed (HCl Suprapur 32%) following trace metal clean procedures. Before sampling, bottles were
129 rinsed three times with the sampled seawater. For the *in situ* measurements, seawater was sampled using a trace metal clean
130 (TMC) rosette equipped with 24 GO-FLO Bottles (Guieu et al., 2020). At each station, 7 to 9 depths were sampled between
131 surface and 1000 m for N_2 fixation measurements, and 5 depths between surface and $\sim 100 \text{ m}$ for primary production
132 measurements (one sample par depth). During the seeding experiments, the six tanks were sampled for simultaneous
133 determination of N_2 - and CO_2 net fixation rates before dust seeding (initial time T0) and one day (T1), two days (T2), and

134 three days (T3) after dust addition at TYR and ION Stations. At FAST, the last sampling took place four days (T4) after dust
135 addition.

136 After collection, 2.3 L of seawater were immediately filtered onto pre-combusted GFF filters to determine natural
137 concentrations and isotopic signatures of particulate organic carbon (POC) and particulate nitrogen (PN). Net N₂ fixation
138 rates were determined using the ¹⁵N₂ gas-tracer addition method (Montoya et al., 1996), and net primary production using the
139 ¹³C-tracer addition method (Hama et al., 1983). Immediately after sampling, 1 mL of NaH¹³CO₃ (99 %, Eurisotop) and 2.5
140 ml of 99 % ¹⁵N₂ (Eurisotop) were introduced to 2.3 L polycarbonate bottles through a butyl septum for simultaneous
141 determination of N₂- and CO₂-fixation. ¹⁵N₂ and ¹³C tracers were added to obtain a ~10 % final enrichment. Then, each bottle
142 was vigorously shaken before incubation for 24 h. The *in situ* samples from the euphotic zone were incubated in on-deck
143 containers with circulating seawater, equipped with blue filters with different sets of blue neutral density filters (Lee Filters)
144 (percentages of attenuation: 70, 52, 38, 25, 14, 7, 4, 2 and 1 %) to simulate an irradiance level (% PAR) as close as possible
145 to the one corresponding to their depth of origin. Samples for N₂ fixation determination in the aphotic layer were incubated
146 in the dark in thermostated incubators set at *in situ* temperature. *In situ* ¹³C-PP will not be discussed in this paper as ¹⁴C-PP
147 rates are presented in Maranon et al. (2021) (see details in Fig. S1). The *in situ* ¹³C-PP and molar C/N ratio in the organic
148 particulate matter, measured simultaneously in our samples (see below for details), were used to estimate the contribution of
149 N₂ fixation to PP.

150 Samples from the dust addition experiments were incubated in two tanks dedicated to incubation: one tank at the same
151 temperature and irradiance as tanks C and D, and another one at the same temperature and irradiance as tanks G. It should be
152 noted that ¹⁴C-PP was also measured during the seedings experiments (Gazeau et al., 2021b).

153 After 24 h incubation, 2.3 L were filtered onto pre-combusted 25 mm GF/F filters, and filters were stored at -25° C. Filters
154 were then dried at 40° C for 48 h before analysis. POC and PN as well as ¹⁵N and ¹³C isotopic ratios were quantified using an
155 online continuous flow elemental analyzer (Flash 2000 HT), coupled with an Isotopic Ratio Mass Spectrometer (Delta V
156 Advantage via a conflow IV interface from Thermo Fischer Scientific). For each sample, POC (in the 0-100m layer) and PN
157 (0-1000m) were higher than the analytically determined detection limit of 0.15 μmol for C and 0.11 μmol for N. Standard
158 deviations were 0.0007 atom% and 0.0005 atom% for ¹³C and ¹⁵N enrichment, respectively. The atom% excess of the
159 dissolved inorganic carbon (DIC) was calculated by using measured DIC concentrations at the LOCEAN laboratory
160 (SNAPO-CO₂). N₂ fixation rates were calculated by isotope mass balance equations as described by Montoya et al. (1996).
161 For each sample, the ¹³C and ¹⁵N uptake rates were considered as significant when excess enrichment of POC and PN was
162 greater than three times the standard deviation obtained on natural samples. According to our experimental conditions, the
163 minimum detectable ¹³C and ¹⁵N uptake rates in our samples were 5 nmol C L⁻¹ d⁻¹ and 0.04 nmol N L⁻¹ d⁻¹, respectively.
164 CO₂ uptake rates were above the detection limit in the upper 0-100m, while N₂ fixation was not quantifiable below 300 m
165 depth except at Stations 1 and 10 with rates ~0.05 nmol N L⁻¹ d⁻¹ at 500 m depth. N₂ fixation rates were calculated by isotope
166 mass balanced as described by Montoya et al. (1996). The detection limit for N₂ fixation, calculated from significant
167 enrichment and lowest particulate nitrogen was 0.04 nmol N L⁻¹ d⁻¹. From these measurements, the molar C:N ratio in the

168 organic particulate matter was calculated and used to estimate the contribution of N₂ fixation to primary production. As a
169 rough estimate of the potential impact of bioavailable N input from N₂ fixation on BP, we used the BP rates presented in
170 companion papers (Gazeau et al., 2021b; Van Wambeke et al., 2021), and converted them in N demand using the molar ratio
171 C/N of 6.8 (Fukuda et al., 1998). Trapezoidal method was used to calculate integrated rates over the SML, the euphotic layer
172 (from surface to 1 % photosynthetically available radiation (PAR) depth) and the 0-1000 m water column.

173 It must be noted that N₂ fixation rates measured by the ¹⁵N₂-tracer gas addition method may have been underestimated due to
174 incomplete ¹⁵N₂ gas bubble equilibration (Mohr et al., 2010). However, this potential underestimation is strongly lowered
175 during long incubation (24h).

176 The relative changes (RC, in %) in N₂ fixation in the dust experiments were calculated as follows :

$$RC (\%) = 100 \times \frac{(N_2FIXATION_{Tx} - N_2FIXATION_{Control})}{(N_2FIXATION_{Control})}$$

177 with N₂ Fixation_{Tx} the rate in D1, D2, G1 or G2 at Tx, N₂ Fixation_{Control} the mean of the duplicated controls (C1 and C2) at
178 Tx, and Tx the time of the sampling.

179

180 **2.4 Composition of the diazotrophic community**

181 Samples for characterization of the diazotrophic communities were collected during the dust seeding experiments in the six
182 tanks at initial time before seeding (T0) and final time (T3 at TYR and ION, and T4 at FAST). Three liters of water were
183 collected in acid-washed containers from each tank, filtered onto 0.2 µm PES filters (Sterivex) and stored at -80° C until
184 DNA extraction. The composition of the diazotrophic community was also determined at four depths (10, 61, 88 and 200 m)
185 at Station 10. Here, 2 L seawater were collected from the TMC rosette. Immediately after collection, seawater was filtered
186 under low vacuum pressure through a 0.2 µm-Nuclepore membrane and stored at -80° C in cryovials. Nucleic acids were
187 obtained from both filter types using phenol-chloroform extraction followed by purification (NucleoSpin® PlantII kit;
188 Macherey-Nagel). DNA extracts were used as templates for PCR amplification of the nifH gene by nested PCR protocol as
189 fully described in Bigeard et al., (2021, protocol.io). Following polymerase chain reactions, DNA amplicons were purified,
190 and quantified using NanoQuant Plate™ and Tecan Spark® (Tecan Trading AG, Switzerland). Each PCR product was
191 normalized to 30ng/µl in final 50µl and sent to Genotoul (<https://www.genotoul.fr/>, Toulouse, France) for high throughput
192 sequencing using paired-end 2x250bp Illumina MiSeq. All reads were processed using the Quantitative Insight Into
193 Microbial Ecology 2 pipeline (QIIME2 v2020.2, Bolyen et al., 2019). Reads were truncated to 350 bp based on sequencing
194 quality, denoised, merged and chimera-checked using DADA2 (Callahan et al., 2016). A total of 1,029,778 reads were
195 assigned to 635 amplicon sequence variants (ASVs). The table was rarefied by filtering at 1 % relative abundance per sample
196 cut-off that reduced the dataset to 97 ASVs accounting for 98.27 % of all reads. Filtering for homologous genes was done
197 using the NifMAP pipeline (Angel et al., 2018) and translation into amino acids using FrameBot (Wang et al., 2013). This
198 yielded 235 ASVs accounting for 1,022,184 reads (99 %). These remaining ASVs were classified with DIAMOND blastp
199 (Buchfink et al 2015) using a FrameBot translated nifH database (phylum level version; Moynihan, 2020) based on the ARB

200 database from the Zehr Lab (version June 2017; <https://www.jzehrlab.com/nifh>). NifH cluster and subcluster designations
201 were assigned according to Frank et al. (2016). UCYN-A sublineages were assigned by comparison to UCYN-A reference
202 sequences (Farnelid et al., 2016; Turk-Kubo et al., 2017). All sequences associated with this study have been deposited
203 under the BioProject ID: PRJNA693966. Alpha and beta-diversity indices for community composition, were estimated after
204 randomized subsampling. Analyses were run in QIIME 2 and in Primer v.6 software package (Clarke and Warwick, 2001).

205

206 **2.5 Complementary data from PEACETIME companions papers**

207 **Bacterial production-** Heterotrophic bacterial production (BP, *sensus stricto* referring to prokaryotic heterotrophic
208 production) was determined on board using the microcentrifuge method with the ³H- leucine (³H-Leu) incorporation
209 technique to measure protein production (Smith and Azam, 1992). The detailed protocol and the rates of BP are presented in
210 Van Wambeke et al. (2021) for measurements in the water column, and in Gazeau et al. (2021b) for measurements over the
211 course of the dust seeding experiments.

212 **Dissolved Fe-** Dissolved iron (DFe) concentrations (< 0.2 μm) were measured by flow injection analysis with online
213 preconcentration and chemiluminescence detection (FIA-CL). The detection limit was 15 pM (Bressac et al., 2021). DFe
214 concentrations in the water column along the whole transect are presented in Bressac et al. (2021) and for the dust seeding
215 experiments in Roy-Barman et al. (2021).

216 **Dissolved inorganic phosphorus and nitrate-** Concentrations of DIP and nitrate (NO₃⁻) were analyzed immediately after
217 collection on 0.2 μm filtered seawater using a segmented flow analyzer (AAIII HR Seal Analytical) according to Aminot and
218 K  rouel (2007) with respective detection limits of 0.02 μmol L⁻¹ and 0.05 μmol L⁻¹. Samples with concentrations below the
219 limit of detection with standard analysis were analyzed by spectrophotometry using a 2.5 m long waveguide capillary cell
220 (LWCC) for DIP (Pulido-Villena et al., 2010) and a 1 m LWCC for NO₃⁻ (Louis et al., 2015); the limit of detection was 1
221 nM for DIP and 6 nM for NO₃⁻. Samples for determination of NO₃⁻ at nanomolar level were lost from Stations 1 to 4. The
222 dust addition experiments data are detailed in Gazeau et al. (2021a). The water column data are fully discussed in Pulido-
223 Villena et al. (2021) and Van Wambeke et al. (2021).

224

225 **2.6 Statistical analysis**

226 Pearson's correlation coefficient was used to test the statistical linear relationship (p < 0.05) between N₂ fixation and other
227 variables (BP, PP, DFe, DIP, NO₃⁻); it should be noted that the DIN stocks estimated at Stations 1 to 4 (Table S1) were
228 excluded from statistical analysis. In the dust seeding experiments, means at initial time (T0) before dust amendment
229 (average at T0 in C and D treatments; n = 4, see Table 2) were compared using a one-way ANOVA followed by a Tukey
230 means comparison test (α = 0.05). When assumptions for ANOVA were not respected, means were compared using a
231 Kruskal-Wallis test and a post hoc Dunn test. To test significant differences (p < 0.05) between the slopes of N₂ fixation as a
232 function of time in the C, D and G treatments (n = 8), an Ancova was performed on data presenting a significant linear

233 relationship with time (Pearson's correlation coefficient, $p < 0.05$). Statistical tests were done using XLSTAT and R (version
234 4.1.1 with the stats, tidyverse and FactoMineR packages).

235

236 **3. Results**

237

238 **3.1 *In situ* N₂ fixation**

239 **3.1.1 Vertical and longitudinal distribution of N₂ fixation**

240 Over the cruise, the water column was well stratified with a shallow SML varying from 7 to 21 m depth (Table S1).
241 Detectable N₂ fixation rates in the 0-1000 m layer ranged from 0.04 to an exceptionally high rate of 72.1 nmol N L⁻¹ d⁻¹ at
242 Station 10 (Fig.2). Vertical N₂ fixation profiles exhibited a similar shape at all stations with maximum values within the
243 euphotic layer and undetectable values below 300 m depth (except at Stations 1 and 10 with rates ~ 0.05 nmol N L⁻¹ d⁻¹ at 500
244 m depth). Within the euphotic layer, all the rates were well above the detection limit (DL = 0.04 nmol N L⁻¹ d⁻¹; minimum *in*
245 *situ* N₂ fixation = 0.22 nmol N L⁻¹ d⁻¹). The highest rates were generally found below the SML and the lowest at the base of
246 the euphotic layer or within the SML (Fig.2). The lowest N₂ fixation rates integrated over the euphotic and aphotic (defined
247 as 1 % PAR depth to 1000 m) layers were found at Station 8, and the highest at Station 10 (Table 1). On average, 59 ± 16 %
248 of N₂ fixation (min 42 % at TYR and ION, max 97 % at Station 10) took place within the euphotic layer (Table 1). The
249 contribution of the SML integrated N₂ fixation to the euphotic layer integrated N₂ fixation was low, on average 17 ± 10 %.
250 Volumetric surface (~ 5 m) and euphotic layer integrated N₂ fixation rates exhibited a longitudinal gradient decreasing
251 eastward ($r = -0.59$ and $r = -0.60$, $p < 0.05$, respectively) (Fig.3). Integrated N₂ fixation rates over the SML, aphotic and 0-
252 1000 m layers (Table 1) displayed no significant trend with longitude ($p > 0.05$). It should be noted that longitudinal trends
253 with stronger correlations were observed for ¹³C-PP and BP ($r = -0.81$ and $r = -0.82$, $p < 0.05$, respectively, Fig.S2) as well as
254 DIP and NO₃⁻ stocks ($r = -0.68$ and $r = -0.85$, $p < 0.05$, no correlation with DFe stock; data not shown) integrated over the
255 euphotic layer.

256

257 **3.1.2 N₂ fixation and composition of diazotrophs at Station 10**

258 The westernmost Station 10 was in sharp contrast to all other stations with an euphotic integrated N₂ fixation on average 44
259 times higher (Table 1) due to high rates of 2.9 at 37 m and 72.1 nmol N L⁻¹ d⁻¹ at 61 m (i.e. at the deep chlorophyll-a
260 maximum, DCM) (Fig.2). That rate at 61 m was associated with a maximum in PP but not with a maximum in BP. From
261 surface to 200 m depth, the *nifH* community composition was largely dominated by ASVs related to different UCYN-A
262 groups (Fig.4) that represented 86 % at 200 m and up to 99.5 % at the DCM. No UCYN-B and -C or filamentous
263 diazotrophs were detected. The relative abundance of NCD (mainly γ -Proteobacteria *Pseudomonas*) increased with depth (r
264 = 0.96, $p < 0.05$) to reach about 8 % in the mesopelagic layer (200 m). UCYN-A1 and -A4 dominated the total diazotrophic
265 community (from 51 to 99 %). All four UCYN-A had different vertical distributions: the relative abundances of UCYN-A1
266 and -A3 were the highest in surface while UCYN-A4 was dominant at the most productive depths (61 and 88 m). At 61 m

267 depth, where the unusually high rate of N₂ fixation was detected, the community was dominated by both UCYN-A4 (58 %)
268 and UCYN-A1 (41 %).

269

270 **3.1.3 N₂ fixation versus primary production, heterotrophic bacterial production, nutrients**

271 For statistical analysis, due to the high integrated N₂ fixation rate from Station 10, this rate was not included in order not to
272 bias the analysis. N₂ fixation rate integrated over the euphotic layer correlated strongly with PP ($r = 0.71$, $p < 0.05$) and BP (r
273 $= 0.76$; $p < 0.05$) (Fig.5). Integrated N₂ fixation over the euphotic layer (and over the SML) was not correlated with the
274 associated DFe, DIP and NO₃⁻ stocks ($p > 0.05$). It should be noted that DIP and NO₃⁻ stocks correlated positively with PP
275 and BP ($p < 0.05$) over the euphotic layer (no correlation between DFe stock, and PP, BP).

276

277 **3.2 Response of N₂ fixation and composition of the diazotrophic communities to dust seeding**

278 **3.2.1 Initial characteristics of the tested seawater**

279 N₂ fixation and BP were the highest at FAST while PP was the highest at FAST and ION (Table 2). The N₂ fixation rates
280 were similar at ION and TYR and significantly higher (factor ~2.6) at FAST. At TYR and ION, the diazotrophs community
281 was largely dominated by NCD (on average 94.5 % of the total diazotrophic community) whereas at FAST, diazotrophic
282 cyanobacteria, mainly UCYN-A, represented on average 91.4 % of the total diazotrophic community. NO₃⁻ concentration
283 was the highest at FAST (59 nM) while DIP concentration was the highest at TYR (17 nM) and the lowest at ION (7 nM).
284 The molar NO₃⁻/DIP ratio was strongly lower than the Redfield ratio (16/1) indicating a potential N limitation of the
285 phytoplanktonic activity in all experiments. DFe concentrations were all higher than 1.5 nM.

286

287 **3.2.2 Changes in N₂ fixation in response to dust seeding and relationship with changes in primary and heterotrophic 288 bacterial production**

289 All the dust seedings led to a significant stimulation of N₂ fixation relative to the controls under present and future climate
290 conditions (D and G treatments) (Figs.6, S3). The reproducibility between the replicated treatments was good at all stations
291 (mean coefficient of variation (CV%) < 14 %). The maximum N₂ fixation relative change (RC) was the highest at TYR
292 (+434-503 % in D1 and D2, +478-565 % in G1 and G2) then at ION (+256-173 % in D1 and D2, and +261-217 % in G1 and
293 G2) and finally at FAST (+41-49 % in D1 and D2 and +97-120 % in G1 and G2) (Fig.7). At TYR and FAST, dust addition
294 stimulated N₂ fixation more in the G treatment than in D, whereas at ION the response was similar between the treatments
295 (Fig.S3). N₂ fixation measured during the dust seeding experiments correlated strongly with PP at FAST ($r = 0.90$, $p < 0.05$),
296 and with BP at TYR and ION ($r > 0.76$, $p < 0.05$) (Fig. S4).

297 **3.2.3 Changes in the diazotrophic composition in response to dust seeding**

298 At TYR and ION, the diazotrophic communities before seeding were largely dominated by NCD (~ 94.5 % of total ASVs,
299 Fig. 8, Table 2). These were mainly γ -proteobacteria related to *Pseudomonas*. Some of these ASVs had low overall relative

300 abundance, and therefore did not appear in the top 20 ASVs (Fig.8; Tables S2, S3) but could nevertheless, account for up to
301 16 % in a specific sample. Filamentous cyanobacteria (*Katagnymene*) were also observed at both stations (~ 4.7 % of the
302 total diazotrophs). The community at FAST was initially dominated by UCYN-A phylotypes, mostly represented by UCYN-
303 A1 and -A3 (relative abundance of UCYN-A1 and -A3 in C and D treatments at T0, n=4 : 34 ± 6 % and 45 ± 2 % of the total
304 diazotrophic composition, respectively, Fig.8). At TYR and ION, the variability at T0 between replicates was higher than at
305 FAST (Fig. S5; C1T0 at TYR was removed due to poor sequencing quality). Also, the diversity (Shannon H') was generally
306 higher at TYR and ION at the start of incubations compared to FAST (T0, Fig.S6). For ION and FAST experiments,
307 *Pseudomonas* related ASVs were more abundant in G treatments at T0 relative to Control and Dust treatments (T0). At the
308 end of the TYR and ION experiments, the community from all treatments appeared to converge (Fig.S5) due to the increase
309 of a few γ -proteobacteria (mainly *Pseudomonas*) that strongly increased in all treatments (Fig.8). At FAST, no difference in
310 the relative abundances of diazotrophs was recorded between D treatment and the controls at T4. However, when comparing
311 G treatment relative to D at T4, the relative contribution of NCD was higher (82 % in G vs. 63 % in D) and the relative
312 abundance of UCYN-A was lower (13 % in G vs. 31 % in D).

313

314 **4. Discussion**

315 Late spring, at the time of sampling, all the stations were well-stratified and characterized by oligotrophic conditions
316 increasing eastward (Maranon et al., 2021; Fig.8 in Guieu et al., 2020). NO_3^- and DIP concentrations were low in the SML,
317 from 9 to 135 nM for NO_3^- (Van Wambeke et al., 2021) and from 4 to 17 nM for DIP (Pulido-Villena et al., 2021); the
318 highest stocks were measured at the westernmost station (St 10) (Table S1).

319

320 **4.1 General features in N_2 fixation and diazotroph community composition**

321 N_2 fixation rates in the aphotic layer were in the range of those previously measured in the western open MS (Benavides et
322 al., 2016) and accounted, on average, for 41 % of N_2 fixation in the 0-1000 m layer, suggesting that a large part of the total
323 diazotrophic activity was related to heterotrophic NCD in the aphotic layer. N_2 fixation rates in the euphotic layer were of the
324 same order of magnitude (data from St10 excluded) than those previously measured in the open MS in spring and summer
325 (Bonnet et al., 2011; Rahav et al., 2013a). At the tested stations, the surface diazotrophic cyanobacteria were largely
326 dominated by UCYN-A (~ 93 % of the total diazotrophic cyanobacteria, mostly UCYN-A1 and -A3) and the NCD
327 community by γ -proteobacteria (~ 95 % of the total NCD). This is the first time that UCYN-A3 and -A4 are detected in the
328 MS. The photo-autotrophic N_2 fixation was negligible as no UCYN-B and -C were detected and very low abundance of
329 filamentous cyanobacteria was observed.

330

331 **4.2 Longitudinal gradient of N_2 fixation related to the composition of the diazotrophic communities**

332 At Station 10 and FAST, the surface diazotrophic communities were largely dominated by UCYN-A (> 91 %) whereas at
333 TYR and ION they were dominated by NCD (> 94 %) which highlights the predominance of photo-heterotrophic

334 diazotrophy in the western waters of the Algerian Basin and of NCD-supported diazotrophy in the Tyrrhenian and Ionian
335 basins. Surface N_2 fixation exhibited a longitudinal gradient decreasing eastward as previously reported (Bonnet et al., 2011,
336 Rahav et al., 2013a). Strong longitudinal gradients decreasing eastward for the relative abundance of UCYN-A ($r = -0.93$, p
337 < 0.05) and inversely increasing eastward for NCD were observed ($r = 0.89$, $p < 0.05$) (Fig.9). Despite no quantitative
338 abundances of distinct diazotrophs for the studied area (in this and previously published studies), the intensity of the bulk N_2
339 fixation rate was likely related to the overall composition of the diazotrophic communities (here relative abundance of
340 UCYN-A versus NCD). Indeed, surface N_2 fixation rates correlated positively with the relative abundance of UCYN-A
341 (mainly A1 and A3) ($r = 0.98$, $p < 0.05$) and negatively with the relative abundance of NCD ($r = -0.99$, $p < 0.05$) (Fig. S7).
342 This could be related, in part, to the variability of the cell-specific N_2 fixation rates that were shown to be higher for UCYN-
343 A relative to NCD (Turk-Kubo et al., 2014; Bentzon-Tilia et al., 2015; Martinez-Perez et al., 2016; Pearl et al., 2018; Mills
344 et al., 2020). Besides, in Atlantic and Pacific Ocean areas when the diazotrophic community is dominated by unicellular
345 organisms, high N_2 fixation rates are mostly associated with a predominance of UCYN-A, and low rates with a
346 predominance of NCD (Turk-Kubo et al., 2014, Martinez-Perez et al., 2016; Moreira-Coello et al., 2017, Fonseca-Batista et
347 al., 2019; Tang et al., 2019).

348

349 **4.3 Intriguing Station 10**

350 The patchy distribution of the diazotrophic activity at Station 10 was related to an exceptionally high rate at the DCM (72.1
351 $nmol N L^{-1} d^{-1}$). High N_2 fixation rates have previously been observed locally: $2.4 nmol N L^{-1} d^{-1}$ at the Strait of Gibraltar
352 (Rahav et al., 2013a), $\sim 5 nmol N L^{-1} d^{-1}$ in the Bay of Calvi (Rees et al., 2017), $17 nmol N L^{-1} d^{-1}$ in the northwestern MS
353 (Garcia et al., 2006) and $129 nmol N L^{-1} d^{-1}$ in the eastern MS (Rees et al., 2006). Station 10 was also hydrodynamically
354 "contrasted" compared to the other stations: it was located almost at the centre of an anticyclonic eddy (Guieu et al., 2020),
355 with the core waters (0-200 m) of Atlantic origin (colder, fresher). In such anticyclonic structures, enhanced exchange with
356 nutrients rich waters from below take place, combined with lateral mixing, could explain higher stocks of NO_3^- and DIP in
357 the euphotic layer (Table S1). Nevertheless, the anomaly of N_2 fixation at the DCM was neither associated with anomalies of
358 PP, BP nor NO_3^- and DIP concentrations. It only coincided with a minimum in DFe concentration ($0.47 nM$ compared to 0.7
359 to $1.4 nM$ at the nearby depths, Bressac et al., 2021). Based on a range of Fe:C (from 7 to $177 \mu mol: mol$) and associated C:N
360 ratios for diazotrophs (*Trichodesmium*, UCYN) from literature (Tuit et al., 2004; Berman-Frank et al., 2007; Jiang et al.,
361 2018), we found that $0.004 nM$ to $0.08 nM$ of DFe are required to sustain this N_2 fixation rate. Consequently, the minimum
362 in DFe concentration at 61m could not be explained solely by the diazotroph uptake.

363

364 Despite no correlation between N_2 fixation and the relative abundance of specific diazotrophs ($p > 0.05$) along the profile,
365 the huge heterogeneity in N_2 fixation rate was likely related to the patchy distribution of diazotrophs taxa. Indeed, patchiness
366 seems to be a common feature of unicellular diazotrophs (Robinart et al., 2014; Moreira-Coello et al., 2019). The
367 exceptionally high N_2 fixation rates coincided with the highest relative contributions of UCYN-A and more precisely

368 UCYN-A4. Exceptional N₂ fixation rates at Station 10, impacted by northeast Atlantic surface waters of subtropical origin
369 could thus be related to that incoming waters. Indeed, Fonseca-Batista et al. (2019) reported high N₂ fixation rates (45 and 65
370 nmol N L⁻¹ d⁻¹ with euphotic N₂ fixation rates up to 1533 μmolN m⁻² d⁻¹) associated with a predominance of UCYN-A in
371 subtropical Atlantic surface water mass along the Iberian Margin (~40° N-11° E). It should be noted that UCYN-A4 was
372 only detected at Station 10, and its relatively high contribution to the whole diazotrophic community in the euphotic layer
373 coincided with the highest stocks of P (and N) (Table S1). This could reflect higher nutrient requirement(s) of the UCYN-A4
374 and/or of its eukaryotic partner relative to other sublineages. Another intriguing feature was the high contribution (~86 %) of
375 UCYN-A in the mesopelagic zone (200 m). As UCYN-A lives in obligate symbiosis with haptophytes from which it
376 receives fixed carbon from photosynthesis (Thompson et al., 2012, 2014), this suggests that this contribution was probably
377 derived from sinking senescing prymnesiophyte-UCYN-A cells, and that the weak N₂ fixation rate at 200m depth is likely
378 only driven by γ-proteobacteria (*Pseudomonas*).

379

380 **4.4 Supply of bioavailable N from diazotrophic activity for fueling primary and heterotrophic bacterial production -** 381 **Relationship with potential controlling factors of N₂ fixation**

382 The relationship established between N₂ fixation, and PP and BP illustrated that in the studied area, N₂ fixation is promoted
383 by UCYN and NCD, and/or could indicate that all processes have the same (co)-limitation. Overall, N₂ fixation was a poor
384 contributor to PP (1.0 ± 0.3 %, Fig. S8), as previously shown in the MS (Bonnet et al., 2011; Yogeve et al., 2011; Rahav et al.
385 2013a) and BP (7 ± 1 %, Fig. S8) except at Station 10 where N₂ fixation could support up to 19 % of PP (Fig. S8) and supply
386 the entire bioavailable N requirements for heterotrophic prokaryotes (199 % of BP). As expected, our results suggest no
387 control of N₂ fixation by DFe and NO₃⁻, as previously shown through nutrient additions in microcosms (Rees et al., 2006;
388 Ridame et al., 2011, Rahav et al., 2016b). No correlation was observed between N₂ fixation and DIP which may highlight the
389 spatial variability of the controlling factor of diazotrophs as DIP was shown to control N₂ fixation in the western basin, but
390 not in the Ionian basin (Ridame et al., 2011). Moreover, DIP concentration does not reflect the rapid turnover of P in the
391 open MS and thus could be a poor indicator of DIP availability (Pulido-Villena et al., 2021).

392

393 **4.5 Diazotrophic activity and composition in response to dust addition under present climate conditions**

394 **General features** – In all experiments, simulated wet dust deposition under present climate conditions triggered a significant
395 (41 to 503 %) and rapid (24-48 h) stimulation of N₂ fixation relative to the controls. Despite this strong increase, N₂ fixation
396 rates remained low (< 0.7 nmol N L⁻¹ d⁻¹) as well as their contribution to PP (< 7 %) and BP (< 5 %) as observed *in situ*
397 (Sect.4.4). All of these results are consistent with those found after dust seeding in mesocosms in a coastal site in the
398 northwestern MS (Ridame et al., 2013) and in the open Cretan Sea (Rahav et al., 2016a).

399 **Temporal Changes in the composition of the diazotrophic community**- Dust addition under present climate conditions did
400 not impact the diazotrophic communities composition. At TYR and ION, the large increase in N₂ fixation recorded after dust
401 addition might be attributed to NCD (mainly γ-proteobacteria), as suggested by the positive correlation between N₂ fixation

402 and BP (Fig S4). At FAST, the community shifted from a large dominance of UCYN-A towards a dominance of NCD both
403 in the dust treatments and unamended controls due to the increase in a few fast growing γ -proteobacteria (mainly
404 *Pseudomonas*). This shift could be attributed to a bottle effect imposed by the tanks which can favor fast growing
405 heterotrophic bacteria (Sherr et al. 1999; Calvo-Diaz et al., 2011). Nevertheless, the increased N_2 fixation after dust seeding
406 at FAST cannot be explained by the shift in composition of the diazotrophic communities because the rates remained quite
407 stable in the controls all along the experiment. Rather, the abundances of diazotrophs have likely increased due to dust input,
408 and UCYN-A in association with prymnesiophytes could still be responsible for the majority of the enhanced N_2 fixation as
409 N_2 fixation correlated strongly with PP (Fig. S4).

410 **Variability of the N_2 fixation response among stations** - The highest stimulation of N_2 fixation to dust addition was
411 observed at TYR (mean $RC_D = 321\%$) then at ION (mean $RC_D = 161\%$) and finally at FAST (mean $RC_D = 21\%$) (Fig.7).
412 The differences in the intensity of the diazotrophic response were not related to differences in the initial nutrients stocks
413 (Table S1) and in the nutrients input from dust which was quite similar between experiments (Gazeau et al., 2021a). Briefly,
414 dust input led to a strong increase of $11.2 \pm 0.2 \mu M NO_3^-$ few hours after seeding in the three experiments, and the maximum
415 DIP release was slightly higher at FAST (31 nM) than at TYR and ION (23 ± 2 nM) (Gazeau et al., 2021a). As DFe
416 concentration before seeding was high (≥ 1.5 nM, Table 2), the bioavailability of Fe did not appear to drive the response of
417 N_2 fixation (Ridame et al., 2013). Also, we evidenced in this experiment that NO_3^- release from dust did not inhibit N_2
418 fixation rate driven by UCYN-A and NCD. This was expected for UCYN-A as it lacks NO_3^- assimilation pathways (Tripp et
419 al., 2010; Bombar et al., 2014).

420 N_2 fixation was initially more limited at TYR and ION (as evidenced by the lowest initial rates) compared to FAST, thereby
421 explaining the highest stimulation of N_2 fixation by dust seeding at these stations. Interestingly, the stimulation of N_2 fixation
422 was higher at TYR than at ION (Fig.7) while these stations presented the same initial rate supported by NCD. One major
423 difference is that PP was not enhanced by dust seeding at TYR while BP increased in both experiments (Gazeau et al.,
424 2021b) suggesting that NCD-supported N_2 fixation was not limited by organic carbon at this station. As N_2 fixation and BP
425 correlated strongly after the dust seeding (Fig. S4), it means that dust-derived DIP could relieve the ambient limitation of
426 both heterotrophic prokaryotes (BP was co-limited by NP, Van Wambeke et al., 2021) and NCD at TYR. This could explain
427 why DIP concentration in the D treatments became again similar to the controls at the end of this experiment (Gazeau et al.,
428 2021a). At ION characterized by the lowest initial DIP concentration, N_2 fixation and PP were likely DIP (co-)limited as
429 shown for BP (Van Wambeke et al., 2021). Consequently, diazotrophs as well as non diazotrophs (heterotrophic prokaryotes
430 and photoautotrophs) could all uptake the dust-derived DIP reducing then potentially the amount of DIP available for each
431 cell that could explain the lower stimulation of N_2 fixation relative to TYR.

432 At FAST, initially dominated by UCYN-A, N_2 fixation and PP correlated strongly after the dust seeding (Fig. S4c). This
433 indicated that dust could relieve either directly the ambient nutrient limitation of both N_2 fixation and PP (Fig.S9) or
434 indirectly through first the relief of the PP limitation of the UCYN-A photoautotroph hosts inducing an increase in the
435 production of organic carbon which could be used by UCYN-A to increase its N_2 -fixing activity. Nutrients from dust could

436 also first enhance the UCYN-A-supported N_2 fixation, which in turn could relieve the N limitation of the UCYN-A
437 photoautotrophic host, as the initial NO_3^-/DIP ratio indicates a potential N limitation of the PP (Table 2).

438

439 **4.6 Response to dust addition under future relative to present climate conditions**

440 **General features** -At TYR and FAST, N_2 fixation was more stimulated by dust input under future than present climate
441 conditions (mean RC_{G-TYR} = 478 % and mean RC_{G-FAST} = 54 %) whereas at ION the response was similar (Figs.7, S3). These
442 differences between future and present climate conditions were not related to the nutrients supplied from dust (Gazeau et al.,
443 2021a).

444 The purpose of our study was to study the combined effect of warming and acidification, but we can expect on the short time
445 scale of our experiments (< 3-4 days), that NCD and UCYN-A would not be directly affected by the changes in the CO_2
446 concentration as they do not fix CO_2 (Zehr et al., 2008). Indeed, no impact of acidification (or pCO_2 increase) on N_2 fixation
447 was detected when the diazotrophic communities were dominated by UCYN-A in the North and South Pacific (Law et al.,
448 2012; Böttjer et al. 2014). Nevertheless, the decrease in pH may indirectly impact UCYN-A through changes affecting its
449 autotrophic host.

450

451 **TYR and ION** -Under future climate conditions, the composition of the diazotrophic communities did not change after dust
452 input at TYR and ION relative to present conditions. At TYR, the highest N_2 fixation stimulation might be linked to the
453 increase in the NCD abundances and/or in their cell-specific N_2 fixation rates under future climate conditions. Unfortunately,
454 the impact of increased temperature and decreased pH on the cell-specific N_2 fixation rates of NCD is currently unknown.
455 However, some studies suggest a positive relationship between temperature and abundances of NCD: diazotrophic γ -
456 proteobacteria (γ -24774A11) gene copies correlated positively with temperature (from ~20 to 30° C) in surface waters of the
457 western South Pacific Ocean (Moisander et al., 2014), and Messer et al. (2015) suggested a temperature optima for these γ -
458 proteobacteria around 25-26° C in the Australian tropical waters. At ION, the similar stimulation of N_2 fixation by dust
459 under future climate conditions compared to present climate conditions could be explained by a greater mortality of
460 diazotrophs due to a higher grazing pressure and/or a higher viral activity. Indeed, higher bacterial mortality in the G
461 treatment that could be related to a higher grazing pressure has been observed (Dinasquet et al., 2021). Another explanation
462 is that in spite of the DIP supply from the dust, the DIP bioavailability, initially the lowest at ION, was not sufficient to allow
463 an additional N_2 fixation stimulation.

464 **FAST**- Some differences in the composition of the diazotrophic communities were observed between present and future
465 climate conditions at FAST after dust input: the contribution of NCD (mainly *Pseudomonas*) increased and that of UCYN-A
466 decreased. It must be noted that the duration of the experiment was longer at FAST (4 days) relative to TYR and ION (3
467 days) which could explain at least partly differences between stations. A direct response of increased temperature and/or
468 decreased pH can be considered on a very short time scale (12 hours) by comparing the results in the G treatment at T0 (+3°
469 C, -0.3 pH unit) with those in C and D treatments. The increased contribution of *Pseudomonas* in the G treatment at T0

470 (before dust addition) reveals a likely positive effect of temperature on the growth of this NCD as an increase in the top-
471 down control on the bacterioplankton was observed after dust seeding under future climate conditions (Dinasquet et al.,
472 2021). Interestingly, despite the decrease in the relative contribution of UCYN-A to the total diazotroph community after
473 dust addition, we observed contrasted responses within the UCYN-A group relative to present climate conditions: the
474 relative abundance of UCYN-A3 strongly decreased (4.6 % in G vs. 25.4 % in D) whereas the relative abundance of UCYN-
475 A2 was twice as high (7 % in G vs. 3.4 % in D). Notably, the relative contribution of UCYN-A1 did not appear to be
476 impacted during the dust addition experiment. These respective changes could be explained by the difference in the
477 temperature tolerance between UCYN-A2 and -A3. Temperature is one of the key drivers explaining the distribution of
478 UCYN-A which appeared to dominate in most of the temperate regions with temperature optima around ~20-24° C
479 (Langlois et al., 2008; Moisaner et al., 2010). However, the temperature optima for the different UCYN-A sublineages, in
480 particular for UCYN-A2 and -A3, are poorly known. Interestingly, Henke et al. (2018) observed that the absolute UCYN-A2
481 abundance was positively affected by increasing temperature, within a range of temperature from about 21 to 28° C which is
482 in agreement with our results although only relative abundances were measured in our study. Based on the strong positive
483 correlation between N₂ fixation and PP after dust addition (and no correlation between N₂ fixation and BP, Fig. S4), and
484 despite the decrease in the relative abundance of UCYN-A3, the increased stimulation of N₂ fixation under future climate
485 conditions could likely be sustained by the increase in the relative abundance of UCYN-A2 which is bigger than UCYN-A3
486 (Cornejo-Castillo et al., 2019) and could consequently have a higher cell-specific N₂ fixation rate.

487

488 **5. Conclusion**

489 In the MS, N₂ fixation is a minor pathway to supply new bioavailable N for sustaining both PP and BP but can locally
490 support up to 20 % of PP and provide all the N requirement for bacterial activity. UCYN-A might be supporting extremely
491 high rates of N₂ fixation (72 nmol.L⁻¹.d⁻¹) in the core of an eddy in the Algerian basin influenced by Atlantic waters. The
492 eastward decreasing longitudinal trend of N₂ fixation in the surface waters is likely related to the spatial variability of the
493 composition of the diazotrophic communities, as shown by the eastward increase in the relative abundance of NCD towards
494 more oligotrophic waters while we observed a westward increase in the relative abundance of UCYN-A. This could reflect
495 lower nutrients requirements for NCD relative to UCYN-A. Through the release of new nutrients, simulated wet dust
496 deposition under present and future climate conditions significantly stimulated N₂ fixation. The degree of stimulation
497 depended on the metabolic activity of the diazotrophs (degree of limitation) related to the composition of diazotrophic
498 communities, and on the ambient potential nutrient limitations of diazotrophs, including that of the UCYN-A
499 prymnesiophyte host. The strongest increase in N₂ fixation, not accompanied with a change in the composition of the
500 diazotrophic communities, was observed at the stations dominated by NCD (TYR, ION) where the nutrient limitation was
501 the strongest. Under projected future levels of temperature and pH, the dust effect is either exacerbated or unchanged.
502 Knowing that NCD and UCYN-A do not fix CO₂, we suggest that, on the time scale of our experiments (3-4 days), the
503 exacerbated response of N₂ fixation is likely the result of the warming (from about 21° C to 24° C) which may increase the

504 growth of NCD when nutrient availability allows it, and may alter the composition of UCYN-A community. However, to
505 date, the effect of acidification and temperature optima of the different UCYN-A sublineages are poorly known (or
506 unknown) as these UCYN-A remain uncultivated.

507 Future changes in climate, desertification and land use practices could induce an increase in dust deposition to the oceans
508 (Tegen et al., 2004; Moulin and Chiapello, 2006; Klingmüller et al., 2016). The predicted future increase in surface
509 temperature, and the resulting stronger stratification are expected to expand the surface of LNLC areas reinforcing
510 consequently the role of new nutrient supply from aeolian dust on the N₂ fixation and probably on the structure of the
511 diazotrophic communities.

512

513 **6. Data availability**

514 Guieu, C. et al. (2020). Biogeochemical dataset collected during the PEACETIME cruise. SEANOE.
515 <https://doi.org/10.17882/75747>.

516

517 **7. Author contributions**

518 FG and CG designed the dust seedings experiments. CR, JD, EB, MB, FVW, FG, VT, AT-S and CG participated to the
519 sampling and analysis. CR and EB performed DNA extraction; EB performed library preparation. CR, JD and SH analyzed
520 the data; CR wrote the manuscript with contributions from all authors.

521

522 **8. Competing interests**

523 The authors declare that they have no conflict of interest

524

525 **9. Special issue Statement**

526 This article is part of the special issue “Atmospheric deposition in the low-nutrient–low-chlorophyll (LNLC) ocean: effects
527 on marine life today and in the future (ACP/BG inter-journal SI)”. It is not associated with a conference.

528

529 **10. Financial support**

530 This study is a contribution to the PEACETIME project (<http://peacetime-project.org>), a joint initiative of the MERMEX and
531 ChArMEx components supported by CNRS-INSU, IFREMER, CEA, and Météo-France as part of the programme
532 MISTRALS coordinated by INSU. PEACETIME was endorsed as a process study by GEOTRACES. JD was funded by a
533 Marie Curie Actions-International Outgoing Fellowship (PIOF-GA-2013-629378). SH and LR were funded by grant 6108-
534 00013 from the Danish Council for independent research to LR.

535

536 **11. Acknowledgments**

537 The authors thank the captain and the crew of the RV Pourquoi Pas ? for their professionalism and their work at sea. We
538 warmly acknowledge our second ‘chieffe’ scientist Karine Desboeufs. We gratefully thank Eric Thiebaut and Pierre
539 Kostyrka for their precious advice with statistical tests. We also thank Kahina Djaoudi and Thibaut Wagener for their
540 assistance in sampling the tanks and TMC-rosette, Magloire Mandeng-Yogo and Fethiye Cetin for IRMS measurements at
541 the Alyses plate-form (SU, IRD). The DIC data used in this study were analyzed at the SNAPO-CO₂ service facility at
542 LOCEAN laboratory and supported by CNRS-INSU and OSU Ecce-Terra

543

544 **12. References**

545 Aminot, A., and K  rouel, R.: Dosage automatique des nutriments dans les eaux marines, in: M  thodes d'analyses en milieu
546 marin, edited by: IFREMER, 188 pp, 2007.

547 Angel, R., Nepel, M., Panh  lzl, C., Schmidt, H., Herbold, C. W., Eichorst, S. A., and Woebken, D.: Evaluation of primers
548 targeting the diazotroph functional gene and development of NifMAP–A bioinformatics pipeline for analyzing nifH
549 amplicon data, *Front. Microbiol.*, 9, 703, <https://doi.org/10.3389/fmicb.2018.00703>, 2018.

550 Bar Zeev, E., Yogev, T., Man-Aharonovich, D., Kress, N., Herut, B., Beja, O., and Berman-Frank, I.: Seasonal dynamics of
551 the endosymbiotic, nitrogen-fixing cyanobacterium *Richelia intracellularis* in the Eastern Mediterranean Sea, *ISME J.*, 2,
552 911–92, <https://doi.org/10.1038/ismej.2008.56>, 2008.

553 Benavides, M., Bonnet, S., Hern  ndez, N., Mart  nez-P  rez, A. M., Nieto-Cid, M., and   lvarez-Salgado, X. A.: Basin-wide
554 N₂ fixation in the deep waters of the Mediterranean Sea, *Global Biogeochem. Cycles*, 30, 952–961,
555 <https://doi.org/10.1002/2015GB005326>, 2016.

556 Bentzon-Tilia, M., Traving, S. J., Mantikci, M., Knudsen-Leerbeck, H., Hansen, J. L. S., Markager, S., and Riemann, L.:
557 Significant N₂ fixation by heterotrophs, photoheterotrophs and heterocystous cyanobacteria in two temperate estuaries,
558 *ISME J.*, 9, <https://doi.org/10.1038/ismej.2014.119273>–85, 2015.

559 Berman-Frank, I.A., Quigg, A., Finkel, Z. V., Irwin, A.J., Haramaty, L.: Nitrogen-fixation strategies and Fe requirements in
560 cyanobacteria, *Limnol. Oceanogr.*, 52, 2260–2269, 2007.

561 Bigeard, E., Lopes Dos Santos, A., and Ribeiro, C.: nifH amplification for Illumina sequencing. [protocols.io](https://dx.doi.org/10.17504/protocols.io.bkiqkudn),
562 <https://dx.doi.org/10.17504/protocols.io.bkiqkudn>, 2021.

563 Bonnet, S., and Guieu, C.: Atmospheric forcing on the annual in the Mediterranean Sea. A one year survey, *J. Geophys.*
564 *Res.*, 111, C09010, <https://doi.org/10.1029/2005JC003213>, 2006.

565 Bonnet, B., Grosso, O., and Moutin, T.: Planktonic dinitrogen fixation along a longitudinal gradient across the
566 Mediterranean Sea during the stratified period (BOUM cruise), *Biogeosciences*, 8, 2257–2267, [https://doi.org/10.5194/bg-8-](https://doi.org/10.5194/bg-8-2257-2011)
567 [2257-2011](https://doi.org/10.5194/bg-8-2257-2011), 2011.

568 Bosc, E., Bricaud, A., and Antoine, D.: Seasonal and interannual variability in algal biomass and primary production in the
569 Mediterranean Sea, as derived from 4 years of SeaWiFS observations, *Global Biogeochem. Cy.*, 18, GB1005,
570 <https://doi.org/10.1029/2003GB002034>, 2004.

571 Bolyen, E., Rideout, J. R., Dillon, M. R., Bokulich, N. A., Abnet, C. C., Al-Ghalith, G. A. et al.: Reproducible, interactive,
572 scalable and extensible microbiome data science using QIIME 2. *Nat. Biotechnol.*, 37, 852–857,
573 <https://doi.org/10.1038/s41587-019-0209-9>, 2019.

574 Bombar, D., Heller, P., Sanchez-Baracaldo, P., Carter, B. J., and Zehr, J.P.: Comparative genomics reveals surprising
575 divergence of two closely related strains of uncultivated UCYN-A cyanobacteria, *ISME J.*, 8, 2530–42,
576 <https://doi.org/10.1038/ismej.2014.167>, 2014.

- 577 Böttjer, D., Karl, D. M., Letelier, R. M., Viviani, D. A., and Church, M. J.: Experimental assessment of diazotroph responses
578 to elevated seawater pCO₂ in the North Pacific Subtropical Gyre, *Global Biogeochem. Cycles*, 28, 601–616,
579 <https://doi.org/10.1002/2013GB004690>, 2014.
- 580 Bressac, M., Wagener, T., Leblond, N., Tovar-Sánchez, A., Ridame, C., Albani, S., Guasco, S., Dufour, A., Jacquet, S.,
581 Dulac, F., Desboeufs, K., and Guieu, C.: Subsurface iron accumulation and rapid aluminium removal in the Mediterranean
582 following African dust deposition, *Biogeosciences Discuss.*, <https://doi.org/10.5194/bg-2021-87>, in review, 2021.
- 583 Buchfink, B., Xie, C., and Huson, D. H.: Fast and sensitive protein alignment using DIAMOND, *Nat. methods*, 12, 1, 59–60,
584 <https://doi.org/10.1038/nmeth.3176>, 2015.
- 585 Callahan, B. J., Mc Murdie, P. J., Rosen, M. J., Han, A. W., Johnson, A. J. A., and Holmes, S.: DADA2: High-resolution
586 sample inference from Illumina amplicon data, *Nat. Methods*, 13, 581, <https://doi.org/10.1038/nmeth.3869>, 2016.
- 587 Clarke, K. R., and Warwick, P. E.: *Change in Marine Communities: An Approach to Statistical Analysis and Interpretation*,
588 Primer-E Ltd: Plymouth, UK, 2001.
- 589 Calvo-Díaz, A., Díaz-Pérez, L., Suárez, L. Á., Morán, X. A. G., Teira, E., and Marañón, E.: Decrease in the autotrophic-to-
590 heterotrophic biomass ratio of picoplankton in oligotrophic marine waters due to bottle enclosure. *Appl. Environ. Microbiol.*,
591 77, 5739–5746, <https://doi.org/10.1128/AEM.00066-11>, 2011.
- 592 Cornejo-Castillo, F. M., Munoz-Marin, M. D. C., Turk-Kubo, K. A., Royo-Llonch, M., Farnelid, H., Acinas, S.G., and Zehr,
593 J.P.: UCYN-A3, a newly characterized open ocean sublineage of the symbiotic N₂-fixing cyanobacterium *candidatus*
594 *Atelocyanobacterium Thalassa*, *Environ. Microbiol.*, 21, 111–24, <https://doi.org/10.1111/1462-2920.14429>, 2019
- 595 Desboeufs, K. V., Losno, R., Colin, J.-L.: Factors influencing aerosol solubility during cloud processes. *Atmos. Environ.*, 35,
596 3529–3537, [https://doi.org/10.1016/S1352-2310\(00\)00472-6](https://doi.org/10.1016/S1352-2310(00)00472-6), 2001.
- 597 Desboeufs, K., Leblond, N., Wagener, T., Bon Nguyen, E., and Guieu, C.: Chemical fate and settling of mineral dust in
598 surface seawater after atmospheric deposition observed from dust seeding experiments in large mesocosms, *Biogeosciences*,
599 11, 5581–5594, <https://doi.org/10.5194/bg-11-5581-2014>, 2014.
- 600 Dinasquet, J., Bigeard, E., Gazeau, F., Azam, F., Guieu, C., Marañón, E., Ridame, C., Van Wambeke, F., Obernosterer, I.,
601 and Baudoux, A.-C.: Impact of dust addition on the microbial food web under present and future conditions of pH and
602 temperature, *Biogeosciences Discuss.*, <https://doi.org/10.5194/bg-2021-143>, in review, 2021.
- 603 D'Ortenzio, F., Iudicone, D., de Boyer Montegut, C., Testor, P., Antoine, D., Marullo, S., Santoleri, R., and Madec, G.:
604 Seasonal variability of the mixed layer depth in the Mediterranean Sea as derived from in situ profiles, *Geophys. Res. Lett.*,
605 32, <https://doi.org/10.1029/2005GL022463>, 2005.
- 606 D'Ortenzio, F., and Ribera d'Alcalà, M.: On the trophic regimes of the Mediterranean Sea: a satellite analysis,
607 *Biogeosciences*, 6, 139–148, <https://doi.org/10.5194/bg-6-139-2009>, 2009.
- 608 Eichner, M., Rost, B., and Kranz, S.: Diversity of ocean acidification effects on marine N₂ fixers, *J. Exp. Mar. Biol. Ecol.*,
609 457, 199–207, <https://doi.org/10.1016/j.jembe.2014.04.015>, 2014.
- 610 El Hourany, R., Abboud-Abi Saab, M., Faour, G., Mejia, C., Crépon, M., and Thiria, S.: Phytoplankton diversity in the
611 Mediterranean Sea from satellite data using self-organizing maps. *J. Geophys. Res-Oceans*, 124,
612 <https://doi.org/10.1029/2019JC015131>, 2019.
- 613 Farnelid, H., Turk-Kubo, K. A., del Carmen Muñoz-Marín, M., and Zehr, J. P.: New insights into the ecology of the globally
614 significant uncultured nitrogen-fixing symbiont UCYN-A, *Aquat. Microb. Ecol.*, 77, 3, 125–138,
615 <https://doi.org/10.3354/ame01794>, 2016.
- 616 Fonseca-Batista, D., Li, X., Riou, V., Michotey, V., Deman, F., Fripiat, F., Guasco, S., Brion, N., Lemaitre, N., Tonnard, M.,
617 Gallinari, M., Planquette, H., Planchon, F., Sarthou, G., Elskens, M., LaRoche, J., Chou, L., and Dehairs, F.: Evidence of
618 high N₂ fixation rates in the temperate northeast Atlantic, *Biogeosciences*, 16, 999–1017, [https://doi.org/10.5194/bg-16-999-](https://doi.org/10.5194/bg-16-999-2019)
619 2019, 2019.

620 Frank, I. E., Turk-Kubo, K. A., and Zehr, J. P.: Rapid annotation of nif H gene sequences using classification and regression
621 trees facilitates environmental functional gene analysis, *Env. microbiol. Rep.*, 8, 5, 905-916. <https://doi.org/10.1111/1758->
622 [2229.12455](https://doi.org/10.1111/1758-2229.12455), 2016.

623 Fu, F.-X., Mulholland, M. R., Garcia, N. S., Beck, A., Bernhardt, P. W., Warner, M. E., Sanudo-Wilhelmy, S. A., and
624 Hutchins, D. A.: Interactions between changing pCO₂, N₂ fixation, and Fe limitation in the marine unicellular
625 cyanobacterium *Crocospaera*, *Limnol. Oceanogr.*, 53, 2472–2484, <https://doi.org/10.4319/lo.2008.53.6.2472>, 2008.

626 Fu, F.-X., Yu, E., Garcia, N. S., Gale, Y., Luo, Y., Webb, E. A., and Hutchins, D.A.: Differing responses of marine N₂ fixers
627 to warming and consequences for future diazotroph community structure, *Aquat. Microb. Ecol.*, 72, 33–46,
628 <https://doi.org/10.3354/ame01683>, 2014.

629 Fukuda, R., Ogawa, H., Nagata, T., and Koike, I.: Direct determination of carbon and nitrogen contents of natural bacterial
630 assemblages in marine environments, *Applied and Environmental Microbiology*, 64(9), 3352–3358.
631 <https://doi.org/10.1128/aem.64.9.3352-3358.1998>, 1998.

632 Garcia, N., Raimbault, P., Gouze, E., and Sandroni, V.: Nitrogen fixation and primary production in Western Mediterranean,
633 *C. R. Biol.*, 329, 742–750, <https://doi.org/10.1016/j.crvi.2006.06.006>, 2006.

634 Gazeau, F., Ridame, C., Van Wambeke, F., Alliouane, S., Stolpe, C., Irisson, J-O., Marro, S., Dolan, J., Blasco, T., Grisoni,
635 J-M., De Liège, G., Hélias-Nunige, S., Djaoudi, K., Pulido-Villena, E., Dinasquet, J., Obernosterer, I., Catala, P., Marie, B.,
636 and Guieu, C.: Impact of dust enrichment on Mediterranean plankton communities under present and future conditions of pH
637 and temperature: an overview, *Biogeosciences*, <https://doi.org/10.5194/bg-2020-202>, 2021a.

638 Gazeau, F., Van Wambeke, F., Marañón, E., Pérez-Lorenzo, M., Alliouane, S., Stolpe, C., Blasco, T., Leblond, N., Zäncker,
639 B., Engel, A., Marie, B., Dinasquet, J., and Guieu, C.: Impact of dust addition on the metabolism of Mediterranean plankton
640 communities and carbon export under present and future conditions of pH and temperature, *Biogeosciences*, 18, 5423–5446,
641 <https://doi.org/10.5194/bg-18-5423-2021>, 2021b.

642 Giorgi, F.: Climate change Hot-spots, *Geophys. Res. Lett.* 33, L08707, <https://doi.org/10.1029/2006GL025734>, 2006.

643 Guieu, C., Dulac, F., Desboeufs, K., Wagener, T., Pulido-Villena, E., Grisoni, J.-M., Louis, F., Ridame, C., Blain, S., Brunet,
644 C., Bon Nguyen, E., Tran, S., Labiadh, M., and Dominici, J.-M.: Large clean mesocosms and simulated dust deposition: a
645 new methodology to investigate responses of marine oligotrophic ecosystems to atmospheric inputs, *Biogeosciences*, 7,
646 [2765-2784](https://doi.org/10.5194/bg-7-2765-2010), <https://doi.org/10.5194/bg-7-2765-2010>, 2010.

647 Guieu, C., and Ridame, C.: Impact of atmospheric deposition on marine chemistry and biogeochemistry, in *Atmospheric*
648 *Chemistry in the Mediterranean Region: Comprehensive Diagnosis and Impacts*, edited by F. Dulac, S. Sauvage, and E.
649 Hamonou, Springer, Cham, Switzerland, 2020.

650 Guieu, C., D'Ortenzio, F., Dulac, F., Taillandier, V., Doglioli, A., Petrenko, A., Barrillon, S., Mallet, M., Nabat, P., and
651 Desboeufs, K.: Introduction: Process studies at the air–sea interface after atmospheric deposition in the Mediterranean Sea –
652 objectives and strategy of the PEACETIME oceanographic campaign (May–June 2017), *Biogeosciences*, 17, 5563–5585,
653 <https://doi.org/10.5194/bg-17-5563-2020>, 2020.

654 Hama, T., Miyazaki, T., Ogawa, Y., Iwakuma, T., Takahashi, M., Otsuki, A., and Ichimura, S.: Measurement of
655 photosynthetic production of a marine phytoplankton population using a stable ¹³C isotope, *Mar. biol.*, 73, 31–36,
656 <https://doi.org/10.1007/BF00396282>, 1983.

657 Henke, B. A., Turk-Kubo, K. A., Bonnet, S., and Zehr, J. P.: Distributions and Abundances of Sublineages of the N₂-Fixing
658 Cyanobacterium *Candidatus Atelocyanobacterium thalassa* (UCYN-A) in the New Caledonian Coral Lagoon, *Front.*
659 *Microbiol.*, 9, 554, <https://doi.org/10.3389/fmicb.2018.00554>, 2018.

660 Herut, B., T. Zohary, M. D. Krom, R. F. Mantoura, P. Pitta, S. Psarra, F. Rassoulzadegan, T. Tanaka, and Thingstad, T. F.:
661 Response of East Mediterranean surface water to Saharan dust: On-board microcosm experiment and field observations,
662 *Deep Sea Res., Part II*, 52, 3024–3040, <https://doi.org/10.1016/j.dsr2.2005.09.003>, 2005.

663 Herut, B., Rahav, E., Tsagaraki, T. M., Giannakourou, A., Tsiola, A., Psarra, S., Lagaria, A., Papageorgiou, N.,
664 Mihalopoulos, N., Theodosi, C. N., Violaki, K., Stathopoulou, E., Scoullou, M., Krom, M. D., Stockdale, A., Shi, Z.,
665 Berman-Frank, I., Meador, T. B., Tanaka, T., and Paraskevi, P.: The potential impact of Saharan dust and polluted aerosols
666 on microbial populations in the East Mediterranean Sea, an overview of a mesocosm experimental approach, *Front. Mar.*
667 *Sci.*, 3, 226, <https://doi.org/10.3389/fmars.2016.00226>, 2016.

668 Hutchins, D., Fu, F-X., Webb, E., Walworth, N., and Tagliabue, A.: Taxon-specific response of marine nitrogen fixers to
669 elevated carbon dioxide concentrations, *Nature Geosci* 6, 790–795, <https://doi.org/10.1038/ngeo1858>, 2013.

670 Ibello, V., Cantoni, C., Cozzi, S., and Civitarese, G.: First basin-wide experimental results on N₂ fixation in the open
671 Mediterranean Sea, *Geophys. Res. Lett.*, 37, L03608, <https://doi.org/10.1029/2009GL041635>, 2010.

672 Ignatiades, L., Gotsis-Skretas, O., Pagou, K., and Krasakopoulou, E.: Diversification of phytoplankton community structure
673 and related parameters along a large-scale longitudinal east-west transect of the Mediterranean Sea, *J. Plankton Res.*, 31,
674 411–428, <https://doi.org/10.1093/plankt/fbn124>, 2009.

675 IPCC: IPCC Special Report on the Ocean and Cryosphere in a Changing Climate, edited by H. O. Pörtner, D. C. Roberts, V.
676 Masson-Delmotte, P. Zhai, M. Tignor, E. Poloczanska, K. Mintenbeck, A. Alegría, M. Nicolai, A. Okem, J. Petzold, B.
677 Rama, and N. M. Weyer., 2019.

678 Jiang, H. B., Fu, F-X., Rivero-Calle, S., Levine, N. M., Sañudo-Wilhelmy, S. A., Qu, P. P., Wang, X. W., Pinedo-Gonzalez,
679 P., Zhu, Z., and Hutchins, D.A.: Ocean warming alleviates iron limitation of marine nitrogen fixation, *Nature Clim. Change*,
680 8, 709–712, <https://doi.org/10.1038/s41558-018-0216-8>, 2018.

681 Klingmüller, K., Pozzer, A., Metzger, S., Stenchikov, G. L., and Lelieveld, J.: Aerosol optical depth trend over the Middle
682 East, *Atmos. Chem. Phys.*, 16, 5063–5073, <https://doi.org/10.5194/acp-16-5063-2016>, 2016.

683 Krom, M. D., Herut, B., and Mantoura, R. F. C.: Nutrient budget for the Eastern Mediterranean: Implications for phosphorus
684 limitation, *Limnol. Oceanogr.*, 49, 1582–1592, <https://doi.org/10.4319/lo.2004.49.5.1582>, 2004.

685 Krom, M. D., Emeis, K. C., and Van Cappellen, P.: Why is the Eastern Mediterranean phosphorus limited?, *Prog. Oceanogr.*,
686 85, 236–244, <https://doi.org/10.1016/j.pocean.2010.03.003>, 2010.

687 Langlois, R. J., Hümmer, D., and LaRoche, J.: Abundances and Distributions of the Dominant nifH Phylotypes in the
688 Northern Atlantic Ocean, *Appl. Env. Microbiol.*, 74, 6, 1922–31, <https://doi.org/10.1128/AEM.01720-07>, 2008.

689 Langlois, R. J., Mills, M. M., Ridame, C., Croot, P., and LaRoche, J.: Diazotrophic bacteria respond to Saharan dust
690 additions, *Mar. Ecol. Prog. Ser.*, 470, 1–14, <https://doi.org/10.3354/meps10109>, 2012.

691 Lazzari, P., Solidoro, C., Ibello, V., Salon, S., Teruzzi, A., Béranger, K., Colella, S., and Crise, A.: Seasonal and inter-annual
692 variability of plankton chlorophyll and primary production in the Mediterranean Sea: a modelling approach, *Biogeosciences*,
693 9, 217–233, <https://doi.org/10.5194/bg-9-217-2012>, 2012.

694 Law, C. S., Breitbarth, E., Hoffmann, L. J., McGraw, C. M. Langlois, R. J., LaRoche, J., Marriner, A., and Safi, K. A.: No
695 stimulation of nitrogen fixation by non-filamentous diazotrophs under elevated CO₂ in the South Pacific, *Glob. Change*
696 *Biol.*, 18, 3004–3014, <https://doi.org/10.1111/j.1365-2486.2012.02777.x>, 2012.

697 Lekunberri, I., Lefort, T., Romero, E., Vázquez-Domínguez, E., Romera-Castillo, C., Marrasé, C., Peters, F., Weinbauer, M.,
698 and Gasol, J. M.: Effects of a dust deposition event on coastal marine microbial abundance and activity, bacterial community
699 structure and ecosystem function, *J. Plankton Res.*, 32, 381–396, <https://doi.org/10.1093/plankt/fbp137>, 2010.

700 Le Moal, M., Collin, H., and Biegala, I.C.: Intriguing diversity among diazotrophic picoplankton along a Mediterranean
701 transect: a dominance of rhizobia, *Biogeosciences*, 8, 827-840, <https://doi.org/10.5194/bg-8-827-2011>, 2011 Louis et al., 2015.

702 Louis, J., Bressac, M., Pedrotti, M. L., and Guieu, C.: Dissolved inorganic nitrogen and phosphorus dynamics in abiotic
703 seawater following an artificial Saharan dust deposition, *Front. Mar. Sci.*, <https://doi.org/10.3389/fmars.2015.00027>, 2015.

704 Manca, B., Burca, M., Giorgetti, A., Coatanoan, C., Garcia, M.-J., and Iona, A.: Physical and biochemical averaged vertical
705 profiles in the Mediterranean regions: An important tool to trace the climatology of water masses and to validate incoming
706 data from operational oceanography, *J. Marine Syst.*, 48, 1–4, 83–116, <https://doi.org/10.1016/j.jmarsys.2003.11.025>, 2004.

707 Man-Aharonovich, D., Kress, N., Bar Zeev, E., Berman-Frank, I., and Beja, O.: Molecular ecology of *nifH* genes and
708 transcripts in the Eastern Mediterranean Sea, *Environ. Microbiol.*, 9, 9, 2354–2363, <https://doi.org/10.1111/j.1462-2920.2007.01353.x>, 2007.

710 Marañón, E., Van Wambeke, F., Uitz, J., Boss, E. S., Pérez-Lorenzo, M., Dinasquet, J., Haëntjens, N., Dimier, C., and
711 Taillandier, V.: Deep maxima of phytoplankton biomass, primary production and bacterial production in the Mediterranean
712 Sea during late spring, *Biogeosciences*, 18, 1749–1767, <https://doi.org/10.5194/bg-18-1749-2021>, 2021.

713 Martinez-Perez, C., Mohr, W., Loscher, C. R., Dekaezemacker, J., Littmann, S., Yilmaz, P., Lehnen, N., Fuchs, B. M.,
714 Lavik, G., Schmitz, R.A., LaRoche, J., and Kuypers, M. M.: The small unicellular diazotrophic symbiont, UCYN-A, is a key
715 player in the marine nitrogen cycle, *Nat. Microbiol.*, 1, 16163, <https://doi.org/10.1038/nmicrobiol.2016.163>, 2016.

716 Mas, J. L., Martin, J., Pham, M. K., Chamizo, E., Miquel, J.-C., Osvath, I., Povinec, P. P., Eriksson, M., and Villa-Alfageme,
717 M.: Analysis of a major Aeolian dust input event and its impact on element fluxes and inventories at the DYFAMED site
718 (Northwestern Mediterranean), *Mar. Chem.*, 223, 103792, <https://doi.org/10.1016/j.marchem.2020.103792>, 2020.

719 Mermex Group, De Madron, X.D., Guieu, C., Sempere, R., Conan, P., Cossa, D., D'Ortenzio, F., Estournel, C., Gazeau, F.,
720 Rabouille, C., Stemmann, L., Bonnet, S., Diaz, F., Koubbi, P., Radakovitch, O., Babin, M., Baklouti, M., Bancon-Montigny,
721 C., Belviso, S., Bensoussan, N., Bonsang, B., Bouloubassi, I., Brunet, C., Cadiou, J.F., Carlotti, F., Chami, M., Charmasson,
722 S., Charriere, B., Dachs, J., Doxaran, D., Dutay, J.C., Elbaz-Poulichet, F., Eleaume, M., Eyrolles, F., Fernandez, C., Fowler,
723 S., Francour, P., Gaertner, J.C., Galzin, R., Gasparini, S., Ghiglione, J.F., Gonzalez, J.L., Goyet, C., Guidi, L., Guizien, K.,
724 Heimbürger, L.E., Jacquet, S.H.M., Jeffrey, W.H., Joux, F., Le Hir, P., Leblanc, K., Lefevre, D., Lejeusne, C., Leme, R.,
725 Loye-Pilot, M.D., Mallet, M., Mejanelle, L., Melin, F., Mellon, C., Merigot, B., Merle, P.L., Migon, C., Miller, W.L.,
726 Mortier, L., Mostajir, B., Mousseau, L., Moutin, T., Para, J., Perez, T., Petrenko, A., Poggiale, J.C., Prieur, L., Pujo-Pay, M.,
727 Pulido, V., Raimbault, P., Rees, A.P., Ridame, C., Rontani, J.F., Pino, D.R., Sicre, M.A., Taillandier, V., Tamburini, C.,
728 Tanaka, T., Taupier-Letage, I., Tedetti, M., Testor, P., Thebault, H., Thouvenin, B., Touratier, F., Tronczynski, J., Ulses, C.,
729 Van Wambeke, F., Vantrepotte, V., Vaz, S., and Verney, R.: Marine ecosystems' responses to climatic and anthropogenic
730 forcings in the Mediterranean, *Prog. Oceanogr.*, 91, 97-166, <https://doi.org/10.1016/j.pocean.2011.02.003>, 2011.

731 Messer, L. F., Doubell, M., Jeffries, T. C., Brown, M. V., and Seymour, J. R.: Prokaryotic and diazotrophic population
732 dynamics within a large oligotrophic inverse estuary, *Aquat. Microb. Ecol.*, 74, 1–15, <https://doi.org/10.3354/ame01726>,
733 2015.

734 Mills, M.M., Turk-Kubo, K.A., van Dijken, G.L., Henke, B.A., Harding, K., Wilson, S.T., Arrigo K.R., and Zehr, J.P.:
735 Unusual marine cyanobacteria/haptophyte symbiosis relies on N₂ fixation even in N-rich environments, *ISME J.*, 14, 2395–
736 2406, <https://doi.org/10.1038/s41396-020-0691-6>, 2020.

737 Moisander, P. H., Beinart, R. A., Hewson, I., White, A. E., Johnson, K. S., Carlson, C. A., Montoya, J. P., and Zehr, J. P.:
738 Unicellular cyanobacterial distributions broaden the oceanic N₂ fixation domain, *Science*, 327, 5972, 1512–1514,
739 <https://doi.org/10.1126/science.1185468>, 2010.

740 Moisander, P. H., Serros, T., Paerl, R. W., Beinart, R. A., Zehr, J. P.: Gammaproteobacterial diazotrophs and *nifH* gene
741 expression in surface waters of the South Pacific Ocean, *ISME J.*, 8, 10, 1962–73, <https://doi.org/10.1038/ismej.2014.49>,
742 2014.

743 Montoya, J. P., Voss, M., Kahler, P., and Capone, D. G.: A simple, high-precision, high-sensitivity tracer assay for N₂
744 fixation, *App. Environ. Microbiol.*, 62, 3, 986-993, <https://doi.org/10.1128/AEM.62.3.986-993.1996>, 1996.

745 Mohr, W., Grosskopf, T., Wallace, D. R. W., and LaRoche, J.: Methodological underestimation of oceanic nitrogen fixation
746 rates, *PLoS One*, 5, 1–7, <https://doi.org/10.1371/journal.pone.0012583>, 2010.

- 747 Moreira-Coello, V., Mouriño-Carballido, B., Marañón, E., Fernández-Carrera, A., Bode, A., and Varela, M. M.: Biological
748 N₂ Fixation in the Upwelling Region off NW Iberia: Magnitude, Relevance, and Players, *Front. Mar. Sci.*, 4, 303,
749 <https://doi.org/10.3389/fmars.2017.00303>, 2017.
- 750 Moreira-Coello, V., Mouriño-Carballido, B., Marañón, E., Fernández-Carrera, A., Bode, A., Sintés, E., Zehr, J.P., Turk-
751 Kubo, K., and Varela, M.M.: Temporal variability of diazotroph community composition in the upwelling region off NW
752 Iberia, *Sci. Rep.*, 9, 3737, <https://doi.org/10.1038/s41598-019-39586-4>, 2019.
- 753 Moulin, C., and Chiapello, I.: Impact of human-induced desertification on the intensification of Sahel dust emission and
754 export over the last decades, *Geophys. Res. Lett.*, 33, <https://doi.org/10.1029/2006GL025923>, 2006.
- 755 Moynihan, M.A.: nifHdada2 GitHub repository, Zenodo, <http://doi.org/10.5281/zenodo.3958370>, 2020
- 756 Paerl, R. W., Hansen, T. N. G., Henriksen, N. S. E., Olesen, A. K., and Riemann, L.: N-fixation and related O₂ constraints
757 on model marine diazotroph *Pseudomonas stutzeri* BAL361, *Aquatic Microbial Ecology*, 81, 125–136,
758 <https://doi.org/10.3354/ame01867>, 2018.
- 759 Pierella Karlusich, J.J., Pelletier, E., Lombard, F., Carsique, M., Dvorak, E., Colin, S., Picheral, M., Cornejo-Castillo, F. M.,
760 Acinas, S. G., Pepperkok, R., Karsenti, E., de Vargas, C., Wincker, P., Bowler, C., and Foster, R. A.: Global distribution
761 patterns of marine nitrogen-fixers by imaging and molecular methods, *Nat. Commun.*, 12, 4160,
762 <https://doi.org/10.1038/s41467-021-24299-y>, 2021.
- 763 Pulido-Villena, E., Wagener, T., and Guieu, C.: Bacterial response to dust pulses in the western Mediterranean: Implications
764 for carbon cycling in the oligotrophic ocean, *Global Biogeochem. Cycles*, 22, GB1020,
765 <https://doi.org/10.1029/2007GB003091>, 2008.
- 766 Pulido-Villena, E., Rérolle, V., and Guieu, C.: Transient fertilizing effect of dust in P-deficient LNLC surface ocean,
767 *Geophys. Res. Lett.*, 37, L01603, <https://doi.org/10.1029/2009GL041415>, 2010.
- 768 Pulido-Villena, E., Baudoux, A. C., Obernosterer, I., Landa, M., Caparros, J., Catala, P., Georges, C., Harmand, J., and
769 Guieu, C.: Microbial food web dynamics in response to a Saharan dust event: results from a mesocosm study in the
770 oligotrophic Mediterranean Sea, *Biogeosciences*, 11, 5607–5619, [10.5194/bg-11-5607-2014](https://doi.org/10.5194/bg-11-5607-2014), 2014.
- 771 Pulido-Villena, E., Desboeufs, K., Djaoudi, K., Van Wambeke, F., Barrillon, S., Doglioli, A., Petrenko, A., Taillandier, V.,
772 Fu, F., Gaillard, T., Guasco, S., Nunige, S., Triquet, S., and Guieu, C.: Phosphorus cycling in the upper waters of the
773 Mediterranean Sea (Peacetime cruise): relative contribution of external and internal sources, *Biogeosciences*, 18, 5871–5889,
774 <https://doi.org/10.5194/bg-18-5871-2021>, 2021.
- 775 Rahav, E., Herut, B., Levi, A., Mulholland, M. R., and Berman-Frank, I.: Springtime contribution of dinitrogen fixation to
776 primary production across the Mediterranean Sea, *Ocean Sci.*, 9, 489–498, <https://doi.org/10.5194/os-9-489-2013>, 2013a.
- 777 Rahav, E., Bar-Zeev, E., Ohayon, S., Elifantz, H., Belkin, N., Herut, B., Mulholland, M. R., and Berman-Frank, I.:
778 Dinitrogen fixation in aphotic oxygenated marine environments, *Front. Microbiol.*, 4, 227,
779 <https://doi.org/10.3389/fmicb.2013.00227>, 2013b.
- 780 Rahav, E., Shun-Yan, C., Cui, G., Liu, H., Tsagaraki, T. M., Giannakourou, A., Tsiola, A., Psarra, S., Lagaria, A.,
781 Mulholland, M. R., Stathopoulou, E., Paraskevi, P., Herut, B., and Berman-Frank, I.: Evaluating the impact of atmospheric
782 depositions on springtime dinitrogen fixation in the Cretan Sea (eastern Mediterranean)—A mesocosm approach, *Front.*
783 *Mar. Sci.*, 3, 180, <https://doi.org/10.3389/fmars.2016.00180>, 2016a.
- 784 Rahav, E., Giannetto, J.M., and Bar-Zeev, E.: Contribution of mono and polysaccharides to heterotrophic N₂ fixation at the
785 eastern Mediterranean coastline, *Sci. Rep.*, 6, 27858, <https://doi.org/10.1038/srep27858>, 2016b.
- 786 Rees, A. P., Law, C. S., and Woodward, E. M. S.: High rates of nitrogen fixation during an in-situ phosphate release
787 experiment in the Eastern Mediterranean Sea, *Geophys. Res. Lett.*, 33, L10607, <https://doi.org/10.1029/2006GL025791>, 2006.

788 Rees, A. P., Turk-Kubo, K. A., Al-Moosawi, L., Alliouane, S., Gazeau, F., Hogan, M. E. and Zehr, J.P.: Ocean acidification
789 impacts on nitrogen fixation in the coastal western Mediterranean Sea, *Estuarine, Coastal and Shelf Science*, 186, Part A, 45-
790 57, <https://doi.org/10.1016/j.ecss.2016.01.020>, 2017.

791 Ridame, C., Le Moal, M., Guieu, C., Ternon, E., Biegala, I. C., L'Helguen, S., and Pujo-Pay M.: Nutrient control of N₂
792 fixation in the oligotrophic Mediterranean Sea and the impact of Saharan dust events, *Biogeosciences*, 8, 2773-
793 2783, <https://doi.org/10.5194/bg-8-2773-2011>, 2011.

794 Ridame, C., Guieu, C., and L'Helguen, S.: Strong stimulation of N₂ fixation in oligotrophic Mediterranean Sea: results from
795 dust addition in large in situ mesocosms, *Biogeosciences*, 10, 7333-7346, <https://doi.org/10.5194/bg-10-7333-2013>, 2013.

796 Ridame, C., Dekaezemacker, J., Guieu, C., Bonnet, S., L'Helguen, S., and Malien, F.: Contrasted Saharan dust events in
797 LNL environments: impact on nutrient dynamics and primary production, *Biogeosciences*, 11, 4783-
798 4800, <https://doi.org/10.5194/bg-11-4783-2014>, 2014.

799 Robidart, J., Church, M., Ryan, J., Ascani, F., Wilson, S. T., Bombar, D., Marin III, R., Richards, K. J., Karl, D. M., Scholin,
800 C. A., and Zehr, J.P.: Ecogenomic sensor reveals controls on N₂-fixing microorganisms in the North Pacific Ocean, *ISME J.*,
801 8, 1175–1185, <https://doi.org/10.1038/ismej.2013.244>, 2014.

802 Roy-Barman, M., Foliot, L., Douville, E., Leblond, N., Gazeau, F., Bressac, M., Wagener, T., Ridame, C., Desboeufs, K.,
803 and Guieu, C.: Contrasted release of insoluble elements (Fe, Al, rare earth elements, Th, Pa) after dust deposition in
804 seawater: a tank experiment approach, *Biogeosciences*, 18, 2663–2678, <https://doi.org/10.5194/bg-18-2663-2021>, 2021.

805 Sherr, E. B., Sherr, B. F., and Sigmon, C. T.: Activity of marine bacteria under incubated and in situ conditions, *Aquatic*
806 *Microbial Ecol.*, 20, 213-223, 1999.

807 Siokou-Frangou, I., Christaki, U., Mazzocchi, M. G., Montesor, M., Ribera d'Alcalá, M., Vaqué, D., and Zingone, A.:
808 Plankton in the open Mediterranean Sea: A review, *Biogeosciences*, 7, 5, 1543–1586, [https://doi.org/10.5194/bg-7-1543-](https://doi.org/10.5194/bg-7-1543-2010)
809 2010, 2010.

810 Smith, D. C. and Azam, F.: A simple, economical method for measuring bacterial protein synthesis rates in sea water using
811 3H-Leucine, *Mar. Microb. Food Webs*, 6, 107-114, 1992.

812 Somot, S., Sevault, F., Deque, M., and Crepon, M.: 21st century climate change scenario for the Mediterranean using a
813 coupled atmosphere – ocean regional climate model, *Global Planet Change*, 63, 112–126,
814 <https://doi.org/10.1016/j.gloplacha.2007.10.003>, 2008.

815 Tang, W., Wang, S., Fonseca-Batista, D., Dehairs, F., Gifford, S., Gonzalez, A. G., Gallinari, M., Planquette, H., Sarthou, G.
816 and Cassar, N.: Revisiting the distribution of oceanic N₂ fixation and estimating diazotrophic contribution to marine
817 production, *Nat. Commun.*, 10, 831, <https://doi.org/10.1038/s41467-019-08640-0>, 2019.

818 Tegen, I., Werner, M., Harrison, S. P., and Kohfeld, K. E.: Relative importance of climate and land use in determining
819 present and future global soil dust emissions, *Geophys. Res. Lett.*, 31, L05105, <https://doi.org/10.1029/2003GL019216>,
820 2004.

821 Ternon E., Guieu, C., Ridame, C., L'Helguen, S., and Catala, P.: Longitudinal variability of the biogeochemical role of
822 Mediterranean aerosols in the Mediterranean Sea, *Biogeosciences*, 8, 1067-1080, <https://doi.org/10.5194/bg-8-1067-2011>,
823 2011.

824 Thompson, A. W., Foster, R. A., Krupke, A., Carter, B. J., Musat, N., Vaultot, D., Kuypers, M. M. M., Zehr, J. P.:
825 Unicellular cyanobacterium symbiotic with a single-celled eukaryotic alga, *Science*, 337, 1546–50.
826 <https://doi.org/10.1126/science.1222700>, 2012.

827 Thompson, A., Carter, B. J., Turk-Kubo, K., Malfatti, F., Azam, F., and Zehr, J. P.: Genetic diversity of the unicellular
828 nitrogen-fixing cyanobacteria UCYN-A and its prymnesiophyte host, *Environ. Microbiol.*, 16, 3238–49,
829 <https://doi.org/10.1111/1462-2920.12490>, 2014.

830 Tovar-Sánchez, A., Rodríguez-Romero, A., Engel, A., Zäncker, B., Fu, F., Marañón, E., Pérez-Lorenzo, M., Bressac, M.,
831 Wagener, T., Triquet, S., Siour, G., Desboeufs, K., and Guieu, C.: Characterizing the surface microlayer in the
832 Mediterranean Sea: trace metal concentrations and microbial plankton abundance, *Biogeosciences*, 17, 2349–2364,
833 <https://doi.org/10.5194/bg-17-2349-2020>, 2020.

834 Tripp, H. J., Bench, S. R., Turk, K. A., Foster, R. A., Desany, B. A., Niazi, F., Affourtit, J. P., and Zehr, J. P.: Metabolic
835 streamlining in an open-ocean nitrogen-fixing cyanobacterium, *Nature*, 464, 90–94, <https://doi.org/10.1038/nature08786>,
836 2010.

837 Tuit, C., Waterbury, J., Ravizza, G.: Diel variation of molybdenum and iron in marine diazotrophic cyanobacteria, *Limnol.*
838 *Oceanogr.*, 49, 978–990, doi:10.4319/lo.2004.49.4.0978, 2004

839 Turk-Kubo, K. A., Farnelid, H. M., Shilova, I. N., Henke, B., and Zehr, J. P.: Distinct ecological niches of marine symbiotic
840 N₂-fixing cyanobacterium *Candidatus Atelocyanobacterium thalassa* sublineages, *J. phycol.*, 53, 2, 451–461,
841 <https://doi.org/10.1111/jpy.12505>, 2017.

842 Turk-Kubo, K. A., Karamchandani, M., Capone, D. G., and Zehr, J.P.: The paradox of marine heterotrophic nitrogen
843 fixation: abundances of heterotrophic diazotrophs do not account for nitrogen fixation rates in the Eastern Tropical South
844 Pacific, *Environmental Microbiology*, 16, 10, 3095–3114, <https://doi.org/doi:10.1111/1462-2920.12346>, 2014.

845 Van Wambeke, F., Taillandier, V., Deboeufs, K., Pulido-Villena, E., Dinasquet, J., Engel, A., Marañón, E., Ridame, C., and
846 Guieu, C.: Influence of atmospheric deposition on biogeochemical cycles in an oligotrophic ocean system, *Biogeosciences*,
847 18, 5699–5717, <https://doi.org/10.5194/bg-18-5699-2021>, 2021.

848 Wang, Q., Quensen, J. F., Fish, J. A., Lee, T. K., Sun, Y., Tiedje, J. M., and Cole, J. R.: Ecological patterns of *nifH* genes in
849 four terrestrial climatic zones explored with targeted metagenomics using FrameBot, a new informatics tool, *MBio*, 4, 5,
850 <https://doi.org/10.1128/mBio.00592-13>, 2013.

851 Webb, E. A., Ehrenreich, I. A., Brown, S. L., Valois, F. W., and Waterbury, J. B.: Phenotypic and genotypic characterization
852 of multiple strains of the diazotrophic cyanobacterium, *Crocospaera watsonii*, isolated from the open ocean, *Env.*
853 *Microbiol.*, 11, 2, 338–348, <https://doi.org/10.1111/j.1462-2920.2008.01771.x>, 2008.

854 Yogeve, T., Rahav, E., Bar-Zeev, E., Man-Aharonovich, D., Stambler, N., Kress, N., Béjà, O., Mulholland, M. R., Herut, B.,
855 and Berman-Frank, I.: Is dinitrogen fixation significant in the Levantine Basin, East Mediterranean Sea?, *Environ.*
856 *Microbiol.*, 13, 4, 854–871, <https://doi.org/10.1111/j.1462-2920.2010.02402.x>, 2011.

857 Zehr, J. P., Mellon, M. T., and Zani, S.: New nitrogen fixing microorganisms detected in oligotrophic oceans by the
858 amplification of nitrogenase (*nifH*) genes, *Appl. Environ. Microbiol.*, 64, 3444–50, [https://doi.org/10.1128/AEM.64.9.3444-](https://doi.org/10.1128/AEM.64.9.3444-3450.1998)
859 [3450.1998](https://doi.org/10.1128/AEM.64.9.3444-3450.1998), 1998.

860 Zehr, J. P., Bench, S. R., Carter, B. J., Hewson, I. and Niazi, F.: Globally Distributed Uncultivated Oceanic N₂-Fixing
861 Cyanobacteria Lack Oxygenic Photosystem II, *Science*, 322, 1110, <https://doi.org/10.1126/science.1165340>, 2008.

862

863

864

865

866

867

868

869

870

871 **Table 1:** Integrated N₂ fixation over the surface mixed layer (SML, from surface to the mixed layer depth), from the surface
872 to the base of the euphotic layer (1% PAR depth), over the aphotic layer (1%PAR depth to 1000 m), and from surface to
873 1000 m at all the sampled stations. Contribution (in %) of SML integrated N₂ fixation to euphotic layer integrated N₂
874 fixation, and contribution of euphotic layer integrated N₂ fixation to total (0-1000 m) integrated N₂ fixation.
875

	N ₂ Fix _{SML}	N ₂ Fix _{euphotic}	N ₂ Fix _{aphotic}	N ₂ Fix _{0-1000m}	N ₂ Fix _{SML} /N ₂ Fix _{euphotic}	N ₂ Fix _{euphotic} /N ₂ Fix 0-1000m
	μmolN m ⁻² d ⁻¹	μmolN m ⁻² d ⁻¹	μmolN m ⁻² d ⁻¹	μmolN m ⁻² d ⁻¹	%	%
ST01	14.6	42.6	56.5	99.1	34	43
ST02	10.7	36.0	16.0	51.9	30	69
ST03	7.8	58.3	18.1	76.4	13	76
ST04	10.8	46.6	38.5	85.1	23	55
ST05	4.9	46.3	36.1	82.4	10	56
TYR	4.2	38.6	53.0	91.6	11	42
ST06	9.1	34.9	29.8	64.7	26	54
ST07	10.5	43.5	55.4	98.8	24	44
ION	6.2	40.6	56.5	97.1	15	42
ST08	4.3	27.0	12.3	39.3	16	69
ST09	3.4	50.2	43.3	93.5	7	54
FAST	5.9	58.2	35.7	93.8	10	62
ST10	13.7	1908	63.7	1972	1	97
Mean ± std (ST10 excluded)	7.7±3.5	44±9	38±16	81±20	18%±9%	55%±12%
Mean ± std (all stations)	8.2±3.7	187±517	40±17	227±525	17%±10%	59%±16%

876

877

878

879

880

881

882

883 **Table 2:** Initial physico-chemical and biological properties of surface seawater before the perturbation in the dust seeding
884 experiments at TYR, ION and FAST (average at T0 in C and D treatments, n=4 or data at T-12h in the pumped surface
885 waters, n=1). The relative abundances of diazotrophic cyanobacteria and NCD (non-cyanobacterial diazotroph) are given as
886 proportion of total *nifH* sequence reads. DIP: dissolved inorganic phosphorus, DFe: dissolved iron. The C:N ratio
887 corresponds to the ratio in the organic particulate matter from IRMS measurements (> 0.7µm). Means that did not differ
888 significantly between the experiments (p>0.05) are labeled with the same letter (in parenthesis).
889

	TYR	ION	FAST
Day of sampling	05/17/2017	05/25/2017	06/02/2017
Temperature (° C)*	20.6	21.2	21.5
Salinity*	37.96	39.02	37.07
¹³ C-Primary production, mg C m ⁻³ d ⁻¹	1.23±0.64 (A)	2.53±0.40 (B)	2.82±0.55 (B)
N ₂ fixation nmol N L ⁻¹ d ⁻¹	0.19±0.03 (A)	0.21±0.05 (A)	0.51±0.04 (B)
Relative abundance of diazotrophic cyanobacteria (%)	4.7±3.8 (A)	6.2±6.5 (A)	91.4±6.0 (B)
Relative abundance of NCD (%)	95.3±3.9 (A)	93.8±6.5 (A)	8.6±6.0 (B)
Heterotrophic bacterial production ng C. L ⁻¹ h ⁻¹	26.6 ± 7.0 (AB)	25.9 ± 0.9 (A)	36.3 ± 1.2 (B)
C:N (mol/mol)	9.6±0.8 (A)	10.2±0.8 (A)	9.1±0.5 (A)
DIP, nM*	17	7	13
NO ₃ ⁻ , nM*	14	18	59
NO ₃ ⁻ /DIP, mol/mol	0.8	2.6	4.5
DFe, nM [§]	1.5±0.1 (A)	2.6±0.2 (B)	1.8±0.2 (A)

890 * from Gazeau et al., 2021a

891 § from Roy-Barman et al., 2021

892

893

894

895

896

897

898

899

900

901

902 **Figures captions**

903 Figure 1: Locations of the ten short (ST1 to ST10) and three long stations (TYR, ION and FAST). Stations 1 and 2 were
904 located in the Provencal basin; Stations 5, 6, and TYR, in the Tyrrhenian Sea; Stations 7, 8, and ION in the Ionian Sea; and
905 Stations 3, 4, 9, 10 and FAST in the Algerian basin. Satellite-derived chlorophyll-a concentration (mg m^{-3}) averaged over the
906 entire duration of the PEACETIME cruise. Ocean color data from MODIS/Aqua, NASA.

907
908 Figure 2: Vertical distribution of N_2 fixation (in $\text{nmol N L}^{-1} \text{d}^{-1}$) in the Provencal (a), Tyrrhenian (b) Ionian (c) and Algerian
909 (d) basins and at Station 10 (e). N_2 fixation rates at Station 10 are plotted in log scale because of the high fluxes. Rates under
910 detection limit ($<0.04 \text{ nmol N L}^{-1} \text{d}^{-1}$) are symbolized by crosses.

911
912 Figure 3: Volumetric surface ($\sim 5\text{m}$) (a) and integrated N_2 fixation from surface to euphotic layer depth (b) along the
913 longitudinal PEACETIME transect (Station 10 was excluded). Integrated N_2 fixation rate from Station 10 was excluded from
914 statistical analysis

915
916 Figure 4: Vertical distribution of the 20 most abundant nifH-ASVs at Station 10, collapsed into major taxonomic groups.

917 Figure 5: N_2 fixation rate integrated over the euphotic layer versus ^{13}C -primary production (a) and bacterial production (b);
918 data at Station 10 were removed.

919
920 Figure 6: N_2 fixation rate in $\text{nmol N L}^{-1} \text{d}^{-1}$ during the dust seeding experiments performed at the stations TYR (a), ION (b)
921 and FAST (c) in the replicated controls (black dot), dust treatments under present climate conditions (red square, D
922 treatment) and dust treatments under future climate conditions (green triangle, G treatment). Open symbols were not
923 included in the linear regression

924
925 Figure 7: Box plots of the relative changes (in %) in N_2 fixation to the rates measured in the controls over the duration of the
926 dust seeding experiments (T1, T2, T3 or T4) at TYR, ION, and FAST stations. D means dust treatments under present
927 climate conditions (D treatment) and G dust treatments under future climate conditions (G treatment). The red cross
928 represents the average.

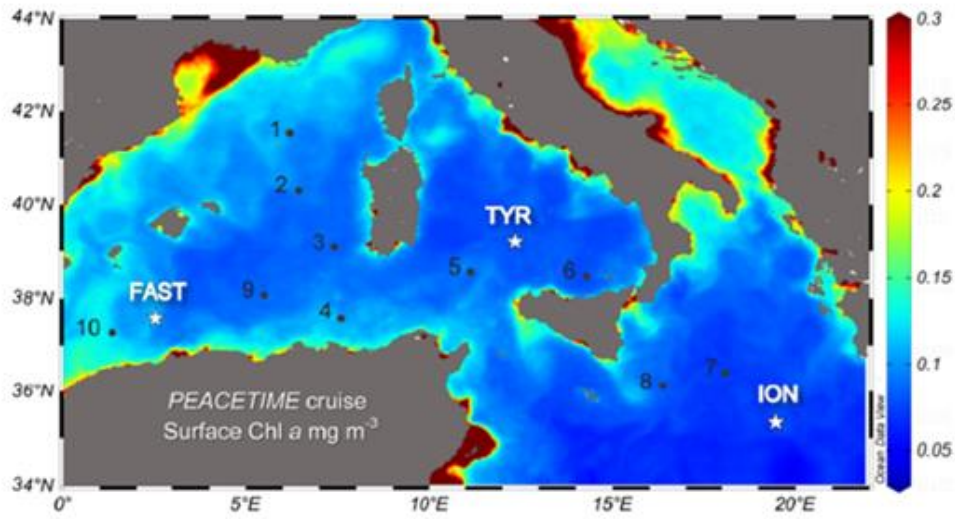
929
930 Figure 8: The composition of diazotrophs (based on 20 most abundant ASVs in the tanks) during the dust seeding
931 experiments at the start (T0) and end (T3 at TYR and ION, and T4 at FAST) in each tank, at TYR (Top panel), ION (middle
932 panel) and FAST (bottom panel). C1T0 at TYR was not included due to poor sequencing quality.

933
934 Figure 9: Relative abundance of the 20 most abundant nifH-ASVs in surface waters (values at TYR, ION and FAST are
935 based on average of duplicated control and dust treatments at T0).

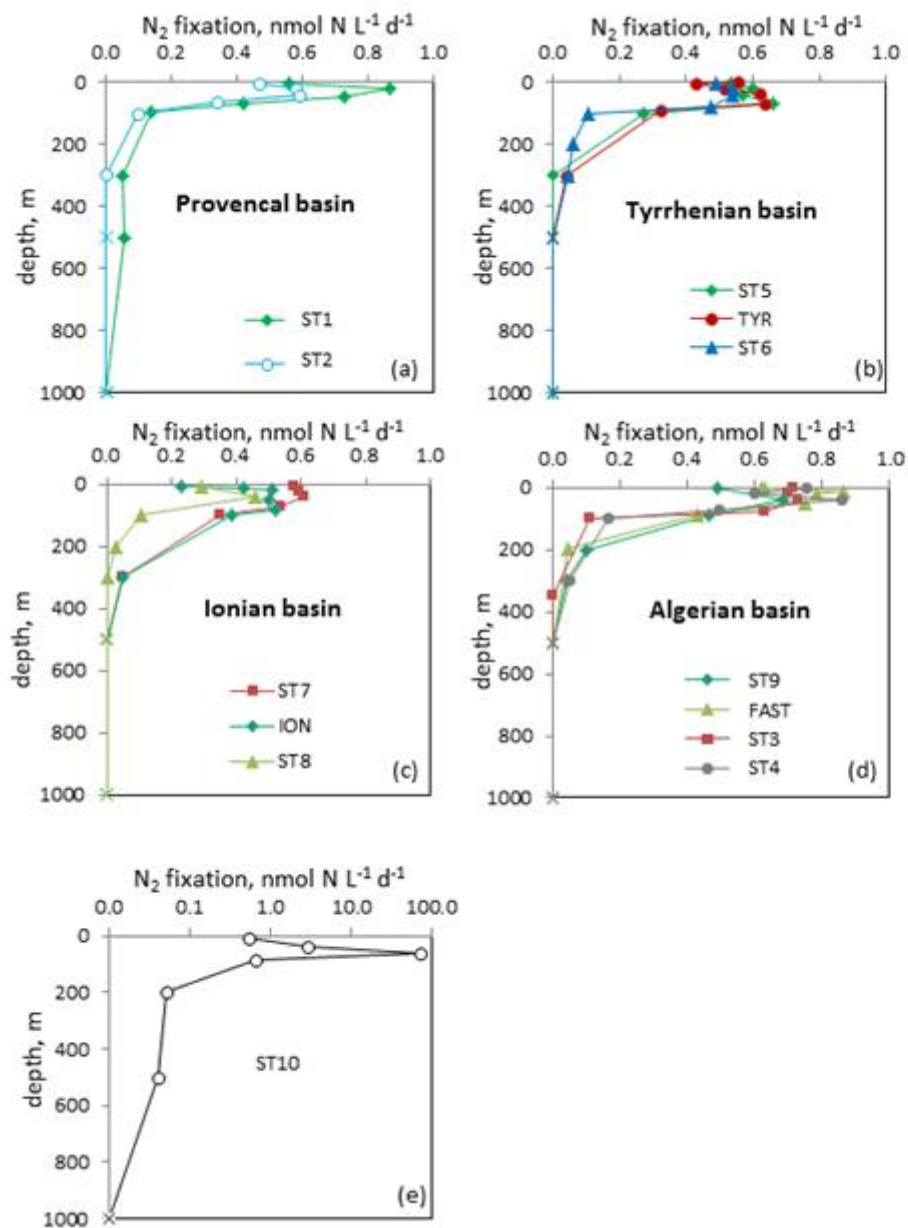
936
937
938
939
940
941
942
943
944
945
946
947
948
949

950
951

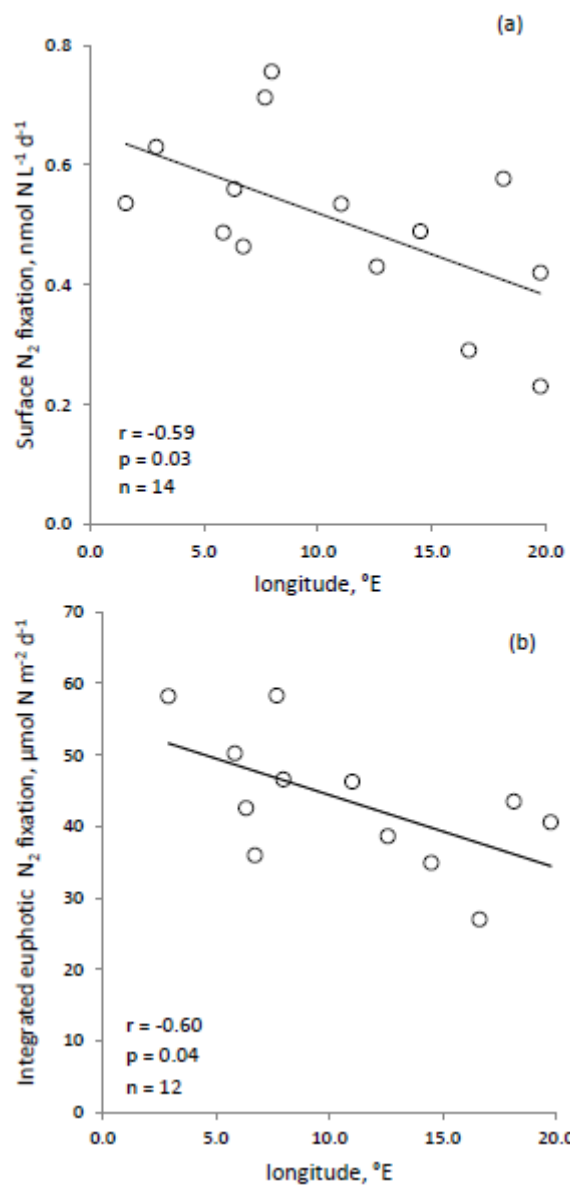
Figure 1 :



952
953
954
955
956
957
958
959
960
961
962
963
964
965
966
967
968



970
 971
 972
 973
 974
 975



977

978

979

980

981

982

983 **Figure 4**

984

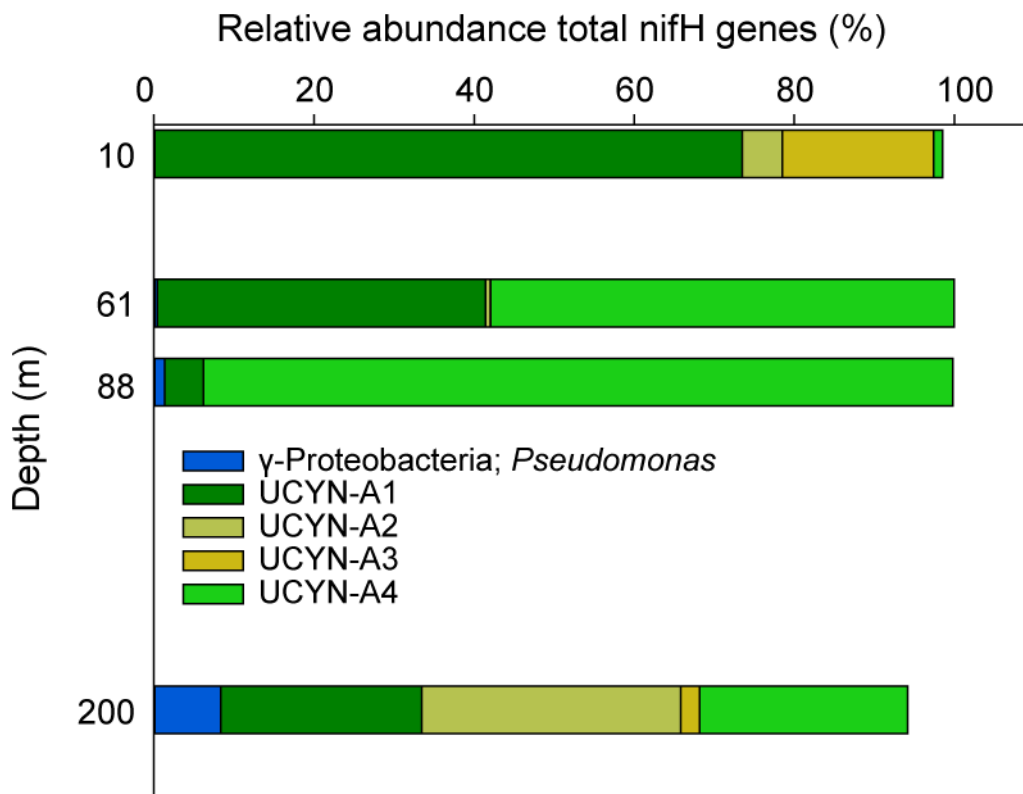
985

986

987

988

989



990

991

992

993

994

995

996

997

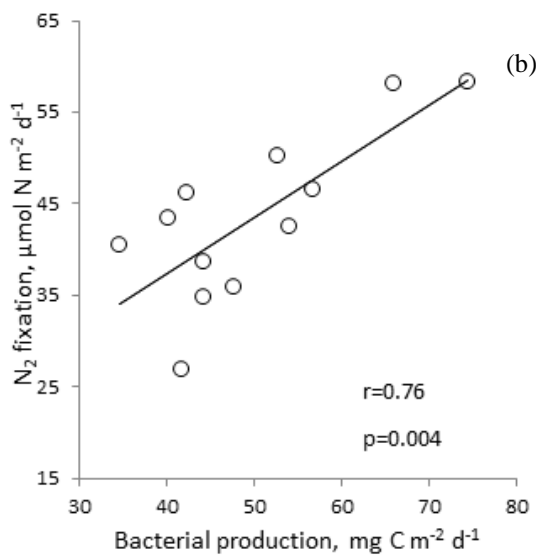
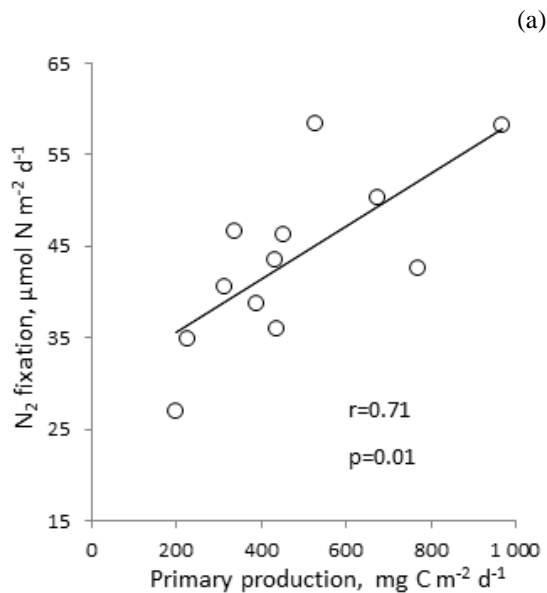
998

999

1000

1001

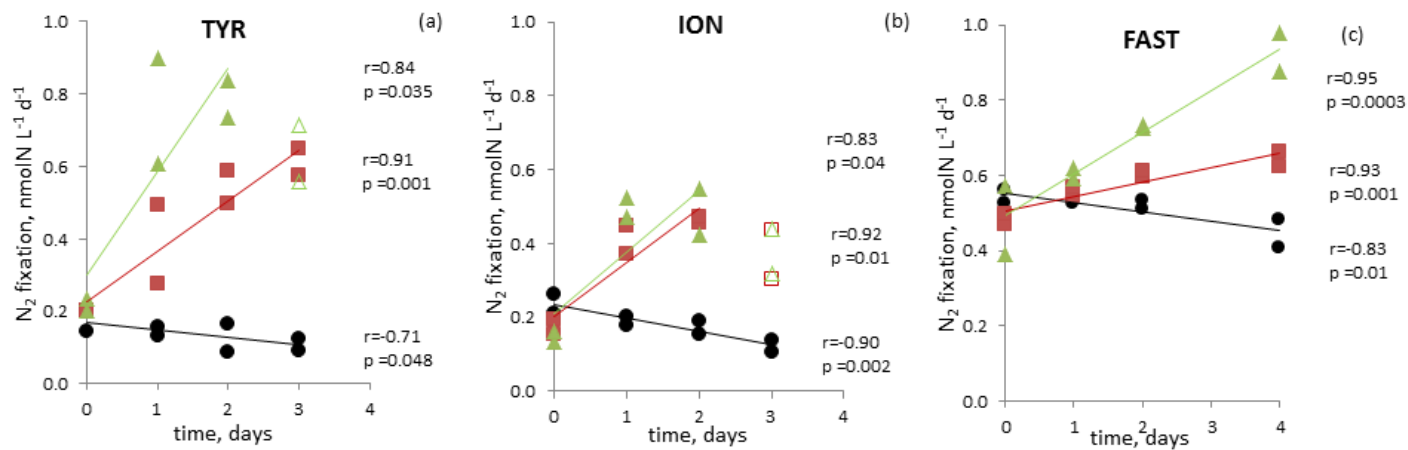
1002



1004
1005
1006
1007
1008
1009

1010
1011
1012

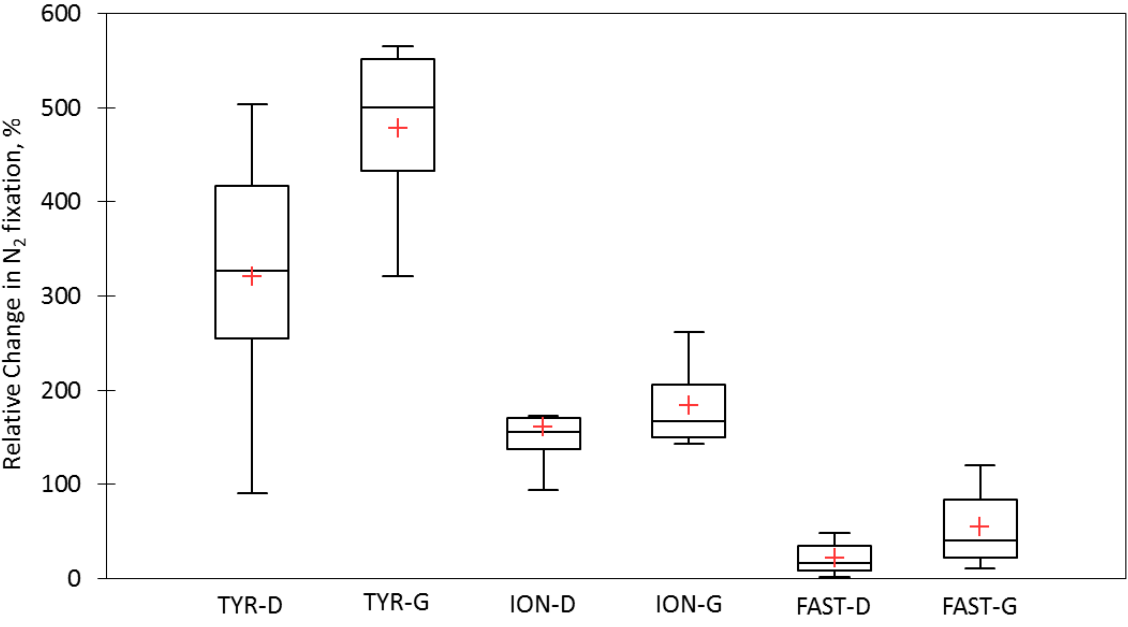
Figure 6



1013
1014
1015
1016
1017
1018
1019
1020
1021
1022
1023
1024
1025
1026
1027
1028
1029
1030
1031
1032
1033
1034

1035 **Figure 7**

1036



1037

1038

1039

1040

1041

1042

1043

1044

1045

1046

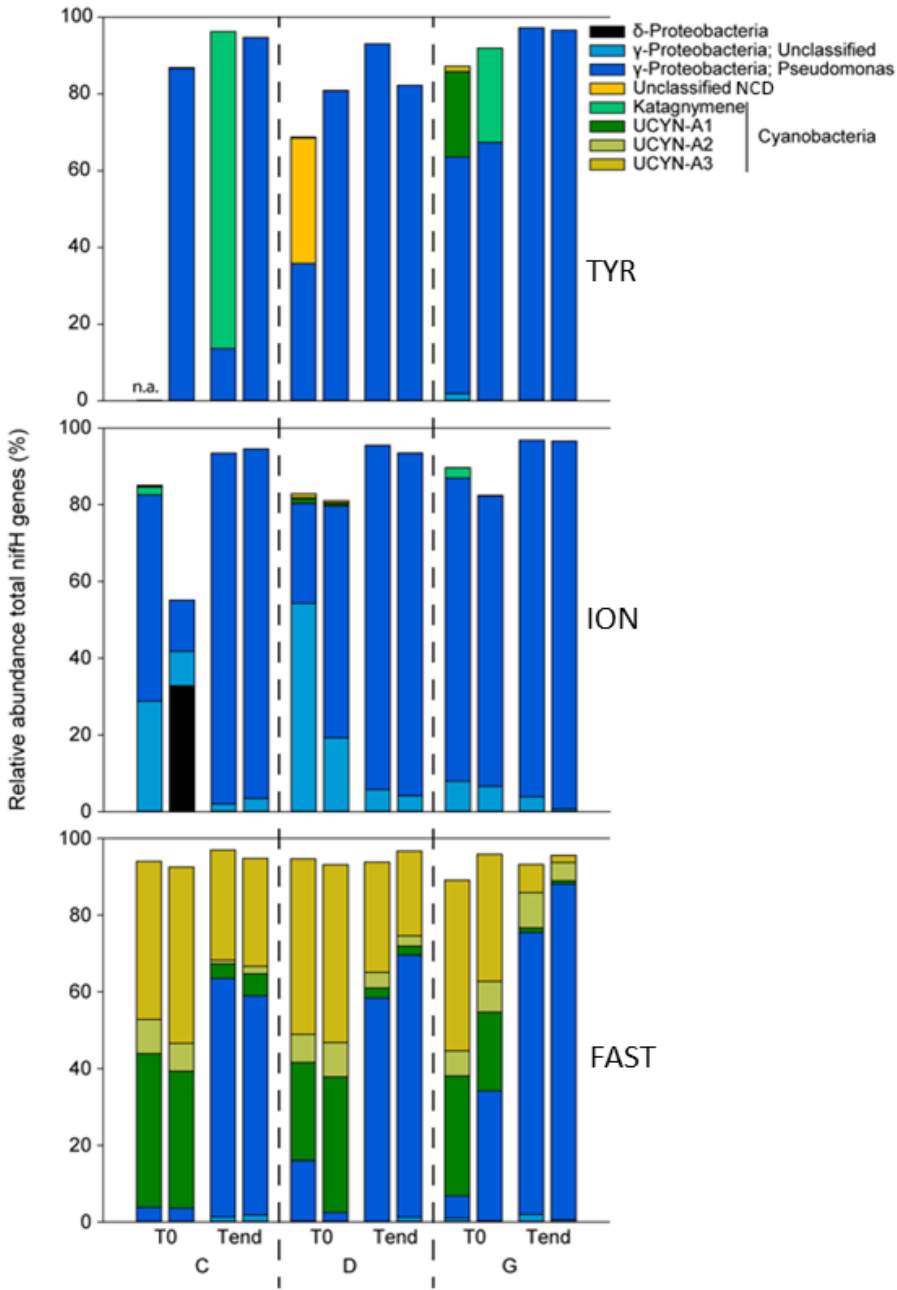
1047

1048

1049

1050

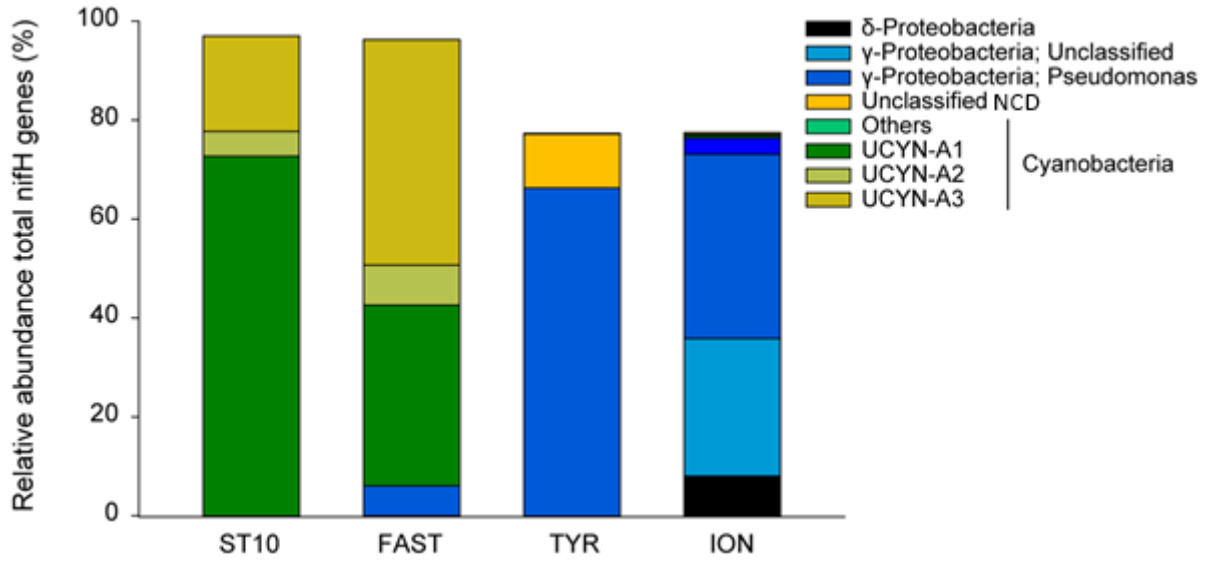
1051



1053
 1054
 1055
 1056

1057
1058
1059
1060
1061

Figure 9



1062
1063
1064
1065
1066
1067
1068
1069
1070
1071
1072
1073
1074
1075
1076
1077
1078
1079
1080
1081
1082